

Superfluidity and Superconductivity in Compact Stars

Nicolas Chamel

Institute of Astronomy and Astrophysics
Université Libre de Bruxelles, Belgium



ULB



NewCompStar School, Bucharest, 20-25 September 2015

Part 2: Superfluidity and superconductivity in neutron stars

Electron superconductivity in neutron stars

The surface layers of non-accreting neutron stars are mostly composed of iron.

Iron is superconducting at density $\rho \simeq 8.2 \text{ g cm}^{-3}$ with $T_c \simeq 2 \text{ K}$, much lower than neutron-star surface temperatures.

Shimizu et al., Nature 412, 316 (2001).



Electron superconductivity in neutron stars

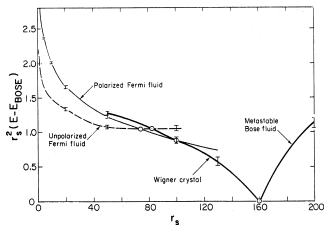
The surface layers of non-accreting neutron stars are mostly composed of iron.

Iron is superconducting at density $\rho \simeq 8.2 \text{ g cm}^{-3}$ with $T_c \simeq 2 \text{ K}$, much lower than neutron-star surface temperatures.

Shimizu et al., Nature 412, 316 (2001).



In the deeper layers of neutron stars at densities $\rho \gtrsim 10^4 \text{ g cm}^{-3}$, atoms are fully ionised. Electrons can be treated as a Fermi gas:



$$r_s \equiv d/a_0$$
$$a_0 \equiv \hbar^2/m_e e^2$$
$$d \equiv (3/4\pi n_e)^{1/3}$$

Ceperley and Alder, PRL45, 566(1980).

In ordinary metals

$$r_s \sim 2 - 6$$

In neutron star crust

$$r_s \sim 10^{-5} - 10^{-2}$$

Electron superconductivity in neutron stars

- The critical temperature of a uniform non-relativistic electron gas in a background of ions (helium) is given by (T_{pi} is the plasma temperature)

$$T_c = T_{\text{pi}} \exp(-8\hbar v_{\text{Fe}}/\pi e^2) \Rightarrow T_c \propto \exp(-\zeta(\rho/\rho_{\text{ord}})^{1/3})$$

with $\rho_{\text{ord}} = m_{\text{u}}/(4\pi a_0^3/3)$.

Therefore T_c decreases with increasing density.

Electron superconductivity in neutron stars

- The critical temperature of a uniform non-relativistic electron gas in a background of ions (jellium) is given by (T_{pi} is the plasma temperature)

$$T_c = T_{\text{pi}} \exp(-8\hbar v_{\text{Fe}}/\pi e^2) \Rightarrow T_c \propto \exp(-\zeta(\rho/\rho_{\text{ord}})^{1/3})$$

with $\rho_{\text{ord}} = m_{\text{u}}/(4\pi a_0^3/3)$.

Therefore T_c decreases with increasing density.

- At densities above $\sim 10^6 \text{ g cm}^{-3}$, electrons become relativistic $v_{\text{Fe}} \sim c$ so that ($\alpha = e^2/\hbar c \simeq 1/137$)

$$T_c = T_{\text{pi}} \exp(-8/\pi\alpha) \sim 0$$

Ginzburg, J. Stat. Phys. 1, 3(1969).

Electron superconductivity in neutron stars

- The critical temperature of a uniform non-relativistic electron gas in a background of ions (jellium) is given by (T_{pi} is the plasma temperature)

$$T_c = T_{\text{pi}} \exp(-8\hbar v_{\text{Fe}}/\pi e^2) \Rightarrow T_c \propto \exp(-\zeta(\rho/\rho_{\text{ord}})^{1/3})$$

with $\rho_{\text{ord}} = m_{\text{u}}/(4\pi a_0^3/3)$.

Therefore T_c decreases with increasing density.

- At densities above $\sim 10^6 \text{ g cm}^{-3}$, electrons become relativistic $v_{\text{Fe}} \sim c$ so that ($\alpha = e^2/\hbar c \simeq 1/137$)

$$T_c = T_{\text{pi}} \exp(-8/\pi\alpha) \sim 0$$

Ginzburg, J. Stat. Phys. 1, 3(1969).

Electrons in neutron stars are not superconducting.

Nuclear superfluidity and superconductivity

The implications of the BCS theory (published in January 1957) for atomic nuclei were first discussed by A. Bohr, B. R. Mottelson, and D. Pines during the Summer of 1957.

D. Pines in "BCS: 50 Years" (World Scientific, 2011), pp.85-105.

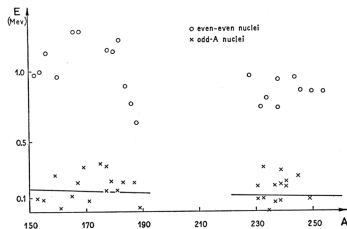
Nuclear superfluidity and superconductivity

The implications of the BCS theory (published in January 1957) for atomic nuclei were first discussed by A. Bohr, B. R. Mottelson, and D. Pines during the Summer of 1957.

D. Pines in "BCS: 50 Years" (World Scientific, 2011), pp.85-105.

A. Bohr, B. R. Mottelson, and D. Pines speculated that nuclear pairing might explain the **energy gap** in the excitation spectra of nuclei.

Phys. Rev. 110, 936 (1958)



They also anticipated that nuclear pairing could explain **odd-even mass staggering**, and the **reduced moments of inertia** of nuclei.

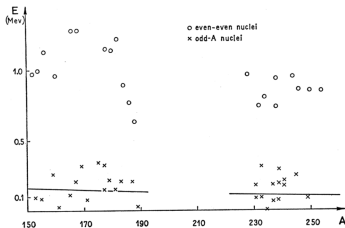
Nuclear superfluidity and superconductivity

The implications of the BCS theory (published in January 1957) for atomic nuclei were first discussed by A. Bohr, B. R. Mottelson, and D. Pines during the Summer of 1957.

D. Pines in "BCS: 50 Years" (World Scientific, 2011), pp.85-105.

A. Bohr, B. R. Mottelson, and D. Pines speculated that nuclear pairing might explain the **energy gap** in the excitation spectra of nuclei.

Phys. Rev. 110, 936 (1958)



They also anticipated that nuclear pairing could explain **odd-even mass staggering**, and the **reduced moments of inertia** of nuclei.

There is however a fundamental difference between nuclei and electrons in solids: **nuclei contain a small number of particles.**

"the present data are insufficient to indicate the limiting value for the gap in a hypothetical infinitely large nucleus." Bohr, Mottelson, Pines.

Superfluidity and superconductivity in neutron stars

Before the discovery of pulsars in 1967, several superconductors were known but only ^4He was found to be superfluid (superfluidity of ^3He was discovered in 1972).



N.N. Bogoliubov, who developed a microscopic theory of superfluidity and superconductivity, was the first to explore its application to nuclear matter.

Dokl. Ak. nauk SSSR 119, 52 (1958).

In 1959, Migdal predicted neutron-star superfluidity, which was first studied by Ginzburg & Kirzhnits in 1964.

Migdal, Nucl. Phys. 13, 655 (1959)

Ginzburg & Kirzhnits, Zh. Eksp. Teor. Fiz. 47, 2006 (1964)

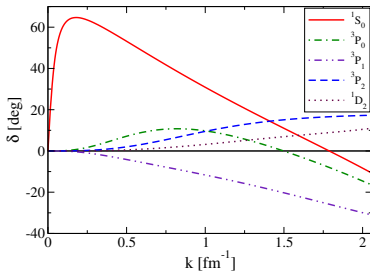
Nuclear superfluidity and superconductivity

At low enough temperatures, nucleons may form pairs that can condense into a superfluid/superconducting phase.

Most attractive pairing channels
($\delta > 0$):

- 1S_0 at low densities
- 3P_2 at high densities

A. Gezerlis, C. J. Pethick, A. Schwenk,
arXiv:1406.6109



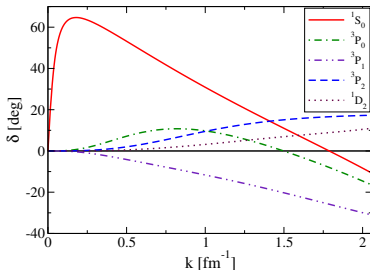
Nuclear superfluidity and superconductivity

At low enough temperatures, nucleons may form pairs that can condense into a superfluid/superconducting phase.

Most attractive pairing channels
($\delta > 0$):

- 1S_0 at low densities
- 3P_2 at high densities

A. Gezerlis, C. J. Pethick, A. Schwenk,
arXiv:1406.6109

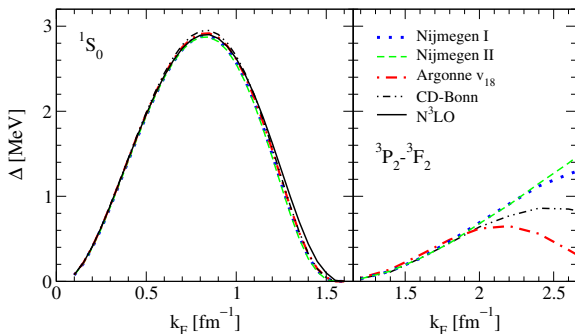


Microscopic calculations of pairing in homogeneous nuclear matter:

- diagrammatic methods
- variational methods
- quantum Monte Carlo methods.

Pairing in neutron matter: BCS

Lowest order approximation: BCS theory.

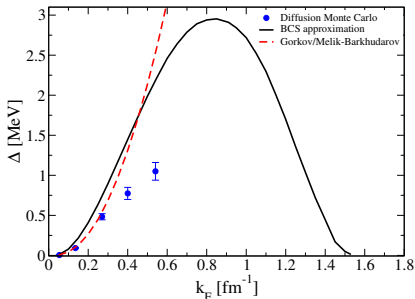


A. Gezerlis, C. J. Pethick, A. Schwenk, *arXiv:1406.6109*

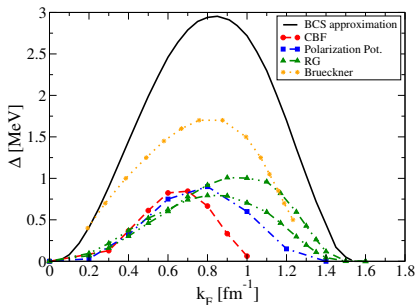
- 1S_0 pairing gaps are essentially independent of the NN potential, the role of the NNN potential is negligible.
- 3P_2 pairing gaps are very dependent on the NN and NNN potentials.

1S_0 pairing in neutron matter: beyond BCS

The 1S_0 pairing gaps are strongly suppressed by medium effects, and to a lesser extent by NNN forces.



A. Gezerlis, C. J. Pethick, A. Schwenk, *arXiv:1406.6109*

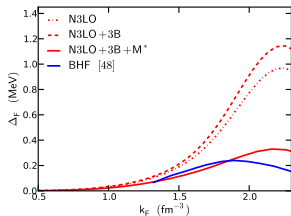
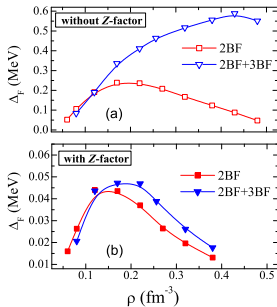
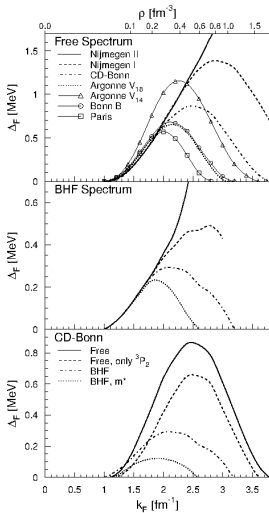


At very low densities, the 1S_0 BCS pairing gap is reduced by a factor $(4 \exp(1))^{-1/3} \simeq 0.45$.

Gorkov&Melik-Barkhudarov, *Sov. Phys. JETP*, 13, 1018, (1961).

3P_2 pairing in neutron matter: beyond BCS

The 3P_2 pairing gaps are also suppressed by medium effects, but are enhanced by NNN forces.



Dong et al., *PRC87*, 062801(R) (2013)

Baldo et al., *PRC58*, 1921 (1998)

Maurizio et al., *PRC90*, 044003 (2014)

Pairing in neutron star cores

The interior of a neutron star is not only made of neutrons, but consists of protons, leptons, hyperons, and possibly mesons, and even deconfined quarks.

Possible phases:

- 1S_0 and 3P_2 proton pairing
- neutron-proton pairing
- hyperon-hyperon pairing ($^1S_0 \Lambda\Lambda$)
- hyperon-nucleon pairing ($^1S_0 n\Lambda$, $^1S_0 n\Sigma^-$, $^3SD_1 n\Sigma^-$)
- quark pairing (see Armen Sedrakian's lecture)

Although 1S_0 proton superconductivity is well established, the other superfluid/superconducting phases have been much less studied.

Pairing in neutron star crusts

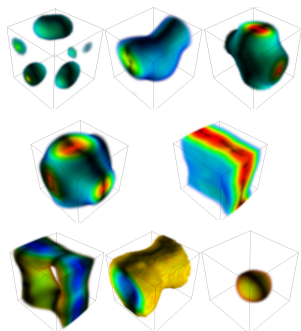
The neutron superfluid in the inner crust of a neutron star coexists with an assembly of neutron-proton clusters, which influence superfluidity.

Because of inhomogeneities, microscopic calculations based on realistic interactions are not feasible.

Phenomenological approaches:

- local density approximation
- semi-classical methods
- self-consistent “mean-field” methods
- beyond “mean-field” methods

All are based on the density functional theory.



*Schuettrumpf et al., PRC87, 055805
(2013)*

Chamel & Haensel, Living Rev. Relativity 11, 10 (2008)

<http://www.livingreviews.org/lrr-2008-10>

Nuclear energy density functional theory in a nut shell

The energy E is expressed as a *functional* of the “**normal**” and “**abnormal**” density matrices:

$$n_q(\mathbf{r}, \sigma; \mathbf{r}', \sigma') = \langle \Psi | c_q(\mathbf{r}'\sigma')^\dagger c_q(\mathbf{r}\sigma) | \Psi \rangle,$$
$$\tilde{n}_q(\mathbf{r}, \sigma; \mathbf{r}', \sigma') = -\sigma' \langle \Psi | c_q(\mathbf{r}' - \sigma') c_q(\mathbf{r}\sigma) | \Psi \rangle$$

where $c_q(\mathbf{r}\sigma)^\dagger$ and $c_q(\mathbf{r}\sigma)$ are the creation and destruction operators for nucleon of type q ($q = n, p$ for neutrons, protons) at position \mathbf{r} with spin σ ($\sigma = \pm 1$ for spin up and down).

Nuclear energy density functional theory in a nut shell

The energy E is expressed as a *functional* of the “**normal**” and “**abnormal**” density matrices:

$$n_q(\mathbf{r}, \sigma; \mathbf{r}', \sigma') = \langle \Psi | c_q(\mathbf{r}'\sigma')^\dagger c_q(\mathbf{r}\sigma) | \Psi \rangle,$$
$$\tilde{n}_q(\mathbf{r}, \sigma; \mathbf{r}', \sigma') = -\sigma' \langle \Psi | c_q(\mathbf{r}' - \sigma') c_q(\mathbf{r}\sigma) | \Psi \rangle$$

where $c_q(\mathbf{r}\sigma)^\dagger$ and $c_q(\mathbf{r}\sigma)$ are the creation and destruction operators for nucleon of type q ($q = n, p$ for neutrons, protons) at position \mathbf{r} with spin σ ($\sigma = \pm 1$ for spin up and down).

In turn the density matrices can be expressed in terms of the **quasiparticle wave functions** $\varphi_{1k}^{(q)}(\mathbf{r})$ and $\varphi_{2k}^{(q)}(\mathbf{r})$ as

$$n_q(\mathbf{r}, \sigma; \mathbf{r}', \sigma') = \sum_{k(q)} \varphi_{2k}^{(q)}(\mathbf{r}, \sigma) \varphi_{2k}^{(q)}(\mathbf{r}', \sigma')^*$$
$$\tilde{n}_q(\mathbf{r}, \sigma; \mathbf{r}', \sigma') = - \sum_{k(q)} \varphi_{2k}^{(q)}(\mathbf{r}, \sigma) \varphi_{1k}^{(q)}(\mathbf{r}', \sigma')^* = - \sum_k \varphi_{1k}^{(q)}(\mathbf{r}, \sigma) \varphi_{2k}^{(q)}(\mathbf{r}', \sigma')^*.$$

Nuclear energy density functional theory in a nut shell

The energy E is expressed as a *functional* of the “**normal**” and “**abnormal**” density matrices:

$$n_q(\mathbf{r}, \sigma; \mathbf{r}', \sigma') = \langle \Psi | c_q(\mathbf{r}'\sigma')^\dagger c_q(\mathbf{r}\sigma) | \Psi \rangle,$$
$$\tilde{n}_q(\mathbf{r}, \sigma; \mathbf{r}', \sigma') = -\sigma' \langle \Psi | c_q(\mathbf{r}' - \sigma') c_q(\mathbf{r}\sigma) | \Psi \rangle$$

where $c_q(\mathbf{r}\sigma)^\dagger$ and $c_q(\mathbf{r}\sigma)$ are the creation and destruction operators for nucleon of type q ($q = n, p$ for neutrons, protons) at position \mathbf{r} with spin σ ($\sigma = \pm 1$ for spin up and down).

In turn the density matrices can be expressed in terms of the **quasiparticle wave functions** $\varphi_{1k}^{(q)}(\mathbf{r})$ and $\varphi_{2k}^{(q)}(\mathbf{r})$ as

$$n_q(\mathbf{r}, \sigma; \mathbf{r}', \sigma') = \sum_{k(q)} \varphi_{2k}^{(q)}(\mathbf{r}, \sigma) \varphi_{2k}^{(q)}(\mathbf{r}', \sigma')^*$$
$$\tilde{n}_q(\mathbf{r}, \sigma; \mathbf{r}', \sigma') = - \sum_{k(q)} \varphi_{2k}^{(q)}(\mathbf{r}, \sigma) \varphi_{1k}^{(q)}(\mathbf{r}', \sigma')^* = - \sum_k \varphi_{1k}^{(q)}(\mathbf{r}, \sigma) \varphi_{2k}^{(q)}(\mathbf{r}', \sigma')^*.$$

The ground-state energy is such as to minimize the functional $E = E[n_q(\mathbf{r}, \sigma; \mathbf{r}', \sigma'), \tilde{n}_q(\mathbf{r}, \sigma; \mathbf{r}', \sigma')]$ under the constraint of fixed nucleon numbers.

Nuclear energy density functional theory in a nut shell

In the simplest cases, E is written as the integral of a *local* functional

$$E = \int \mathcal{E} \left[n_q(\mathbf{r}), \nabla n_q(\mathbf{r}), \tau_q(\mathbf{r}), \mathbf{J}_q(\mathbf{r}), \tilde{n}_q(\mathbf{r}) \right] d^3\mathbf{r}$$

where

$$\begin{aligned} n_q(\mathbf{r}) &= \sum_{\sigma=\pm 1} n_q(\mathbf{r}, \sigma; \mathbf{r}, \sigma) \\ \tau_q(\mathbf{r}) &= \sum_{\sigma=\pm 1} \int d^3\mathbf{r}' \delta(\mathbf{r} - \mathbf{r}') \nabla \cdot \nabla' n_q(\mathbf{r}, \sigma; \mathbf{r}', \sigma) \\ \mathbf{J}_q(\mathbf{r}) &= -i \sum_{\sigma, \sigma'=\pm 1} \int d^3\mathbf{r}' \delta(\mathbf{r} - \mathbf{r}') \nabla n_q(\mathbf{r}, \sigma; \mathbf{r}', \sigma') \times \boldsymbol{\sigma}_{\sigma\sigma'} \\ \tilde{n}_q(\mathbf{r}) &= \sum_{\sigma=\pm 1} \tilde{n}_q(\mathbf{r}, \sigma; \mathbf{r}, \sigma) \end{aligned}$$

and $\boldsymbol{\sigma}_{\sigma\sigma'}$ denotes the Pauli spin matrices.

Duguet, Lecture Notes in Physics 879 (Springer-Verlag, 2014), p. 293

Dobaczewski & Nazarewicz, in "50 years of Nuclear BCS" (World Scientific Publishing, 2013), pp.40-60

Nuclear energy density functional theory in a nut shell

Minimizing $E \left[\varphi_{1k}^{(q)}(\mathbf{r}), \varphi_{2k}^{(q)}(\mathbf{r}) \right]$ under the constraint of fixed nucleon numbers lead to the **Hartree-Fock-Bogoliubov equations** (analogous to Bogoliubov-de Gennes equations for superconductors):

$$\sum_{\sigma'} \begin{pmatrix} h_q(\mathbf{r})_{\sigma\sigma'} & \Delta_q(\mathbf{r})\delta_{\sigma\sigma'} \\ \Delta_q(\mathbf{r})\delta_{\sigma\sigma'} & -h_q(\mathbf{r})_{\sigma\sigma'} \end{pmatrix} \begin{pmatrix} \varphi_{1k}^{(q)}(\mathbf{r}, \sigma') \\ \varphi_{2k}^{(q)}(\mathbf{r}, \sigma') \end{pmatrix} = E_k \begin{pmatrix} \varphi_{1k}^{(q)}(\mathbf{r}, \sigma) \\ \varphi_{2k}^{(q)}(\mathbf{r}, \sigma) \end{pmatrix}$$

$$h_q(\mathbf{r})_{\sigma'\sigma} \equiv -\nabla \cdot \frac{\delta E}{\delta \tau_q(\mathbf{r})} \nabla \delta_{\sigma\sigma'} + \frac{\delta E}{\delta n_q(\mathbf{r})} \delta_{\sigma\sigma'} - i \frac{\delta E}{\delta \mathbf{J}_q(\mathbf{r})} \cdot \nabla \times \boldsymbol{\sigma}_{\sigma'\sigma} - \mu_q \delta_{\sigma\sigma'},$$

μ_q are the chemical potentials (Lagrange multipliers),

$\Delta_q(\mathbf{r}) \equiv \frac{\delta E}{\delta \tilde{n}_q(\mathbf{r})}$ is called the pair potential or the **pairing field**.

With suitable boundary conditions, these equations can not only describe the bulk neutron superfluid in neutron-star crusts, but also quantized vortices.

Intermission: functional derivative

Let us consider that the energy $E[n(\mathbf{r})]$ is a functional of the density $n(\mathbf{r})$ and its gradient.

Intermission: functional derivative

Let us consider that the energy $E[n(\mathbf{r})]$ is a functional of the density $n(\mathbf{r})$ and its gradient.

The functional derivative is defined by

$$\delta E = \int d^3r \frac{\delta E}{\delta n(\mathbf{r})} \delta n(\mathbf{r}) \equiv \lim_{\epsilon \rightarrow 0} \frac{E[n(\mathbf{r}) + \epsilon \delta n(\mathbf{r})] - E[n(\mathbf{r})]}{\epsilon} = \left. \frac{dE}{d\epsilon} \right|_{\epsilon=0}$$

where $\delta n(\mathbf{r})$ is an *arbitrary* variation of the density that vanishes at the boundary of the integration domain.

Intermission: functional derivative

Let us consider that the energy $E[n(\mathbf{r})]$ is a functional of the density $n(\mathbf{r})$ and its gradient.

The functional derivative is defined by

$$\delta E = \int d^3r \frac{\delta E}{\delta n(\mathbf{r})} \delta n(\mathbf{r}) \equiv \lim_{\epsilon \rightarrow 0} \frac{E[n(\mathbf{r}) + \epsilon \delta n(\mathbf{r})] - E[n(\mathbf{r})]}{\epsilon} = \left. \frac{dE}{d\epsilon} \right|_{\epsilon=0}$$

where $\delta n(\mathbf{r})$ is an *arbitrary* variation of the density that vanishes at the boundary of the integration domain.

Example: $E[n(\mathbf{r})] = \int d^3r \mathcal{E}(\mathbf{r})$ with $\mathcal{E}(\mathbf{r}) = \mathcal{E}(n(\mathbf{r}), \nabla n(\mathbf{r}))$

$$\frac{\delta E}{\delta n(\mathbf{r})} = \frac{\partial \mathcal{E}(\mathbf{r})}{\partial n(\mathbf{r})} - \nabla \cdot \frac{\partial \mathcal{E}(\mathbf{r})}{\partial \nabla n(\mathbf{r})}$$

Effective nuclear energy density functional

- **In principle, the nuclear functional can be inferred from realistic NN interactions** (i.e. fitted to experimental NN phase shifts) using many-body methods

$$\mathcal{E} = \frac{\hbar^2}{2M}(\tau_n + \tau_p) + A(\rho_n, \rho_p) + B(\rho_n, \rho_p)\tau_n + B(\rho_p, \rho_n)\tau_p$$

$$+ C(\rho_n, \rho_p)(\nabla\rho_n)^2 + C(\rho_p, \rho_n)(\nabla\rho_p)^2 + D(\rho_n, \rho_p)(\nabla\rho_n) \cdot (\nabla\rho_p)$$

+ Coulomb, spin-orbit and pairing

Drut, Furnstahl and Platter, Prog.Part.Nucl.Phys.64(2010)120.

Effective nuclear energy density functional

- **In principle, the nuclear functional can be inferred from realistic NN interactions** (i.e. fitted to experimental NN phase shifts) using many-body methods

$$\mathcal{E} = \frac{\hbar^2}{2M}(\tau_n + \tau_p) + A(\rho_n, \rho_p) + B(\rho_n, \rho_p)\tau_n + B(\rho_p, \rho_n)\tau_p$$

$$+ C(\rho_n, \rho_p)(\nabla\rho_n)^2 + C(\rho_p, \rho_n)(\nabla\rho_p)^2 + D(\rho_n, \rho_p)(\nabla\rho_n) \cdot (\nabla\rho_p)$$

+ Coulomb, spin-orbit and pairing

Drut, Furnstahl and Platter, Prog.Part.Nucl.Phys.64(2010)120.

- **But this is a very difficult task** so in practice, phenomenological functionals are employed.
Bender, Heenen and Reinhard, Rev.Mod.Phys.75, 121 (2003).
Bulgac in "50 years of Nuclear BCS" (World Scientific Publishing, 2013), pp.100-110

Effective nucleon-nucleon interaction

Semi-local functionals can be constructed from **Skyrme effective nucleon-nucleon interactions** of the form

$$\begin{aligned} v_{ij} = & t_0(1 + x_0 P_\sigma) \delta(\mathbf{r}_{ij}) + \frac{1}{2} t_1(1 + x_1 P_\sigma) \frac{1}{\hbar^2} [p_{ij}^2 \delta(\mathbf{r}_{ij}) + \delta(\mathbf{r}_{ij}) p_{ij}^2] \\ & + t_2(1 + x_2 P_\sigma) \frac{1}{\hbar^2} \mathbf{p}_{ij} \cdot \delta(\mathbf{r}_{ij}) \mathbf{p}_{ij} + \frac{1}{6} t_3(1 + x_3 P_\sigma) \rho(\mathbf{r})^\alpha \delta(\mathbf{r}_{ij}) \\ & + \frac{i}{\hbar^2} W_0 (\boldsymbol{\sigma}_i + \boldsymbol{\sigma}_j) \cdot \mathbf{p}_{ij} \times \delta(\mathbf{r}_{ij}) \mathbf{p}_{ij} \end{aligned}$$

using the “**mean-field**” approximation, where $\mathbf{r}_{ij} = \mathbf{r}_i - \mathbf{r}_j$, $\mathbf{r} = (\mathbf{r}_i + \mathbf{r}_j)/2$, $\mathbf{p}_{ij} = -i\hbar(\nabla_i - \nabla_j)/2$ is the relative momentum, and P_σ is the two-body spin-exchange operator.

The parameters t_i , x_i , α , W_0 are fitted to some experimental and/or microscopic nuclear data.

Remark: fitting directly the energy functional \mathcal{E} (to nuclear-matter calculations for instance) may lead to self-interaction errors.

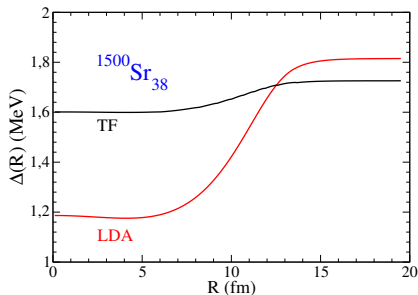
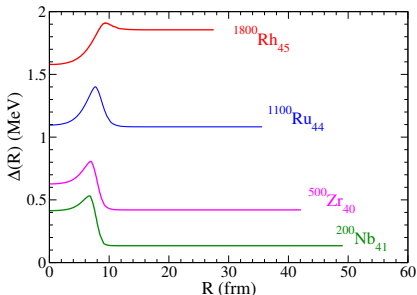
Chamel, Phys. Rev. C 82, 061307(R) (2010).

Semi-classical methods

- **Local density approximation** ($\xi \ll \ell$)
assuming matter is locally homogeneous: $\Delta(\mathbf{r}) = \Delta(n_n(\mathbf{r}), n_p(\mathbf{r}))$

Semi-classical methods

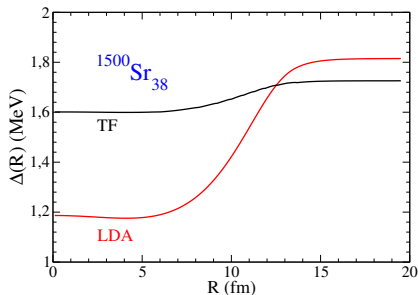
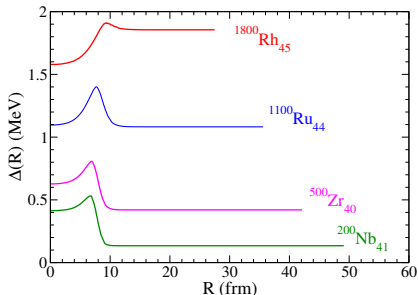
- **Local density approximation** ($\xi \ll \ell$)
assuming matter is locally homogeneous: $\Delta(\mathbf{r}) = \Delta(n_n(\mathbf{r}), n_p(\mathbf{r}))$
- **Semi-classical approximation** ($\lambda_F \ll \ell$)
 $\hbar \rightarrow 0$ limit of the BCS gap equation



Schuck & Vinas, in "50 years of nuclear BCS" (World Scientific Publishing, 2013), pp. 212-226

Semi-classical methods

- **Local density approximation** ($\xi \ll \ell$)
assuming matter is locally homogeneous: $\Delta(\mathbf{r}) = \Delta(n_n(\mathbf{r}), n_p(\mathbf{r}))$
- **Semi-classical approximation** ($\lambda_F \ll \ell$)
 $\hbar \rightarrow 0$ limit of the BCS gap equation



Schuck & Vinas, in "50 years of nuclear BCS" (World Scientific Publishing, 2013), pp. 212-226

Superfluidity is **highly non-local** due to proximity effects (the coherence length is large compared to spatial density fluctuations). But quantum effects are not fully taken into account.

Band theory

Floquet-Bloch theorem

I found to my delight that the wave differed from the plane wave of free electrons only by a periodic modulation.

Bloch, Physics Today 29 (1976), 23-27.

Band theory

Floquet-Bloch theorem

I found to my delight that the wave differed from the plane wave of free electrons only by a periodic modulation.

Bloch, Physics Today 29 (1976), 23-27.



The single-particle wave functions can be expressed as

$$\varphi_{\alpha\mathbf{k}}(\mathbf{r}) = e^{i\mathbf{k}\cdot\mathbf{r}} u_{\alpha\mathbf{k}}(\mathbf{r})$$

where $u_{\alpha\mathbf{k}}(\mathbf{r} + \boldsymbol{\ell}) = u_{\alpha\mathbf{k}}(\mathbf{r})$ and $\boldsymbol{\ell}$ are lattice vectors.

Band theory

Floquet-Bloch theorem

I found to my delight that the wave differed from the plane wave of free electrons only by a periodic modulation.

Bloch, Physics Today 29 (1976), 23-27.



The single-particle wave functions can be expressed as

$$\varphi_{\alpha\mathbf{k}}(\mathbf{r}) = e^{i\mathbf{k}\cdot\mathbf{r}} u_{\alpha\mathbf{k}}(\mathbf{r})$$

where $u_{\alpha\mathbf{k}}(\mathbf{r} + \boldsymbol{\ell}) = u_{\alpha\mathbf{k}}(\mathbf{r})$ and $\boldsymbol{\ell}$ are lattice vectors.

- α (band index) accounts for the rotational symmetry around each lattice site,
- \mathbf{k} (wave vector) accounts for the translational symmetry of the crystal.

Chamel, Goriely, Pearson, in "50 years of Nuclear BCS" (World Scientific Publishing, 2013), pp.284-296.

Band theory

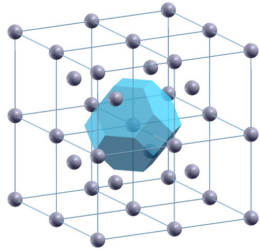
By symmetry, the crystal can be partitioned into identical primitive cells. The HFB equations need to be solved only inside one cell.

Band theory

By symmetry, the crystal can be partitioned into identical primitive cells. The HFB equations need to be solved only inside one cell.

- The shape of the cell depends on the crystal symmetry

Example : body centered
cubic lattice

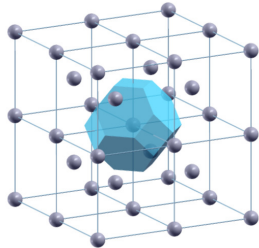


Band theory

By symmetry, the crystal can be partitioned into identical primitive cells. The HFB equations need to be solved only inside one cell.

- The shape of the cell depends on the crystal symmetry

Example : body centered cubic lattice



- The boundary conditions are fixed by the Floquet-Bloch theorem

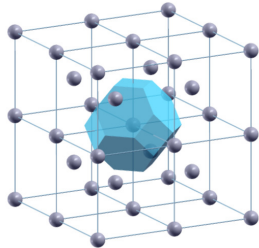
$$\varphi_{\alpha\mathbf{k}}(\mathbf{r} + \boldsymbol{\ell}) = e^{i\mathbf{k}\cdot\boldsymbol{\ell}} \varphi_{\alpha\mathbf{k}}(\mathbf{r})$$

Band theory

By symmetry, the crystal can be partitioned into identical primitive cells. The HFB equations need to be solved only inside one cell.

- The shape of the cell depends on the crystal symmetry

Example : body centered cubic lattice



- The boundary conditions are fixed by the Floquet-Bloch theorem

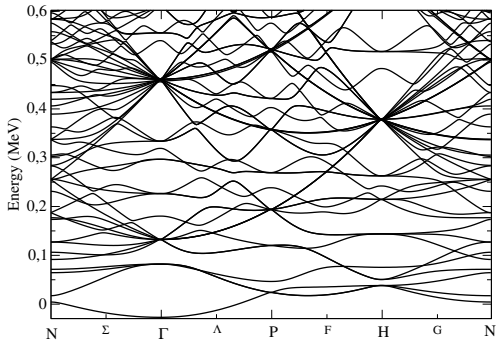
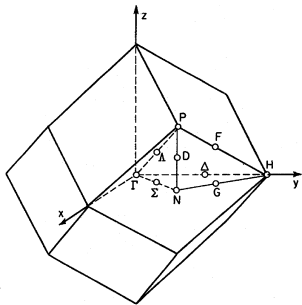
$$\varphi_{\alpha\mathbf{k}}(\mathbf{r} + \boldsymbol{\ell}) = e^{i\mathbf{k}\cdot\boldsymbol{\ell}} \varphi_{\alpha\mathbf{k}}(\mathbf{r})$$

- \mathbf{k} can be restricted to the first Brillouin zone (primitive cell of the reciprocal lattice) since for any reciprocal lattice vector \mathbf{K}

$$\varphi_{\alpha\mathbf{k}+\mathbf{K}}(\mathbf{r}) = \varphi_{\alpha\mathbf{k}}(\mathbf{r})$$

Example of neutron band structure

Body-centered cubic crystal of zirconium like clusters with $N = 160$
(70 unbound) and $\bar{\rho} = 7 \times 10^{11} \text{ g.cm}^{-3}$



Chamel et al, Phys.Rev.C75 (2007), 055806

Anisotropic multi-band neutron superfluidity

In the deep layers of neutron-star crusts, the spatial fluctuations of $\Delta(\mathbf{r})$ are small compared to $\varphi_{\alpha\mathbf{k}}(\mathbf{r})$ so that

$$\int d^3\mathbf{r} \varphi_{\alpha\mathbf{k}}^*(\mathbf{r}) \Delta(\mathbf{r}) \varphi_{\beta\mathbf{k}}(\mathbf{r}) \approx \delta_{\alpha\beta} \int d^3\mathbf{r} |\varphi_{\alpha\mathbf{k}}(\mathbf{r})|^2 \Delta(\mathbf{r}).$$

Anisotropic multi-band neutron superfluidity

In the deep layers of neutron-star crusts, the spatial fluctuations of $\Delta(\mathbf{r})$ are small compared to $\varphi_{\alpha\mathbf{k}}(\mathbf{r})$ so that

$$\int d^3\mathbf{r} \varphi_{\alpha\mathbf{k}}^*(\mathbf{r}) \Delta(\mathbf{r}) \varphi_{\beta\mathbf{k}}(\mathbf{r}) \approx \delta_{\alpha\beta} \int d^3\mathbf{r} |\varphi_{\alpha\mathbf{k}}(\mathbf{r})|^2 \Delta(\mathbf{r}).$$

In this decoupling approximation, the Hartree-Fock-Bogoliubov equations reduce to the BCS equations

$$\Delta_{\alpha\mathbf{k}} = -\frac{1}{2} \sum_{\beta} \sum_{\mathbf{k}'} \bar{v}_{\alpha\mathbf{k}\beta\mathbf{k}'}^{\text{pair}} \frac{\Delta_{\beta\mathbf{k}'}}{E_{\beta\mathbf{k}'}} \tanh \frac{E_{\beta\mathbf{k}'}}{2k_B T}$$

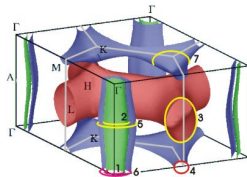
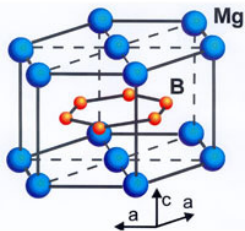
$$\bar{v}_{\alpha\mathbf{k}\beta\mathbf{k}'}^{\text{pair}} = \int d^3\mathbf{r} v^{\pi}[\rho_n(\mathbf{r}), \rho_p(\mathbf{r})] |\varphi_{\alpha\mathbf{k}}(\mathbf{r})|^2 |\varphi_{\beta\mathbf{k}'}(\mathbf{r})|^2$$

$$E_{\alpha\mathbf{k}} = \sqrt{(\varepsilon_{\alpha\mathbf{k}} - \mu)^2 + \Delta_{\alpha\mathbf{k}}^2}$$

$\varepsilon_{\alpha\mathbf{k}}$, μ and $\varphi_{\alpha\mathbf{k}}(\mathbf{r})$ are obtained from band structure calculations.
Chamel et al., Phys.Rev.C81,045804 (2010).

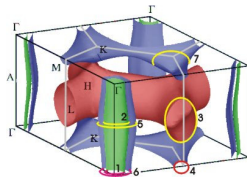
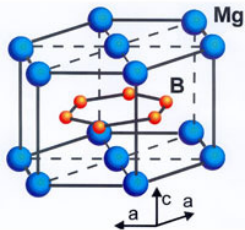
Analogy with terrestrial multi-band superconductors

Multi-band superconductors were first studied by Suhl et al. in 1959 but clear evidence were found only in 2001 with the discovery of MgB_2 (two-band superconductor)



Analogy with terrestrial multi-band superconductors

Multi-band superconductors were first studied by Suhl et al. in 1959 but clear evidence were found only in 2001 with the discovery of MgB_2 (two-band superconductor)

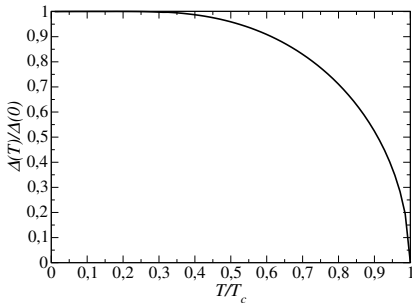
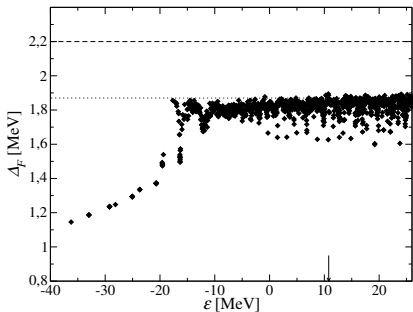


In neutron-star crusts,

- the number of bands can be huge \sim up to a thousand!
- both intra- and inter-band couplings must be taken into account

Neutron pairing gaps

Example at $\bar{n} = 0.06 \text{ fm}^{-3}$ with BSk16



- $\Delta_{\alpha k}(T)/\Delta_{\alpha k}(0)$ is a universal function of T
- The critical temperature is approximately given by the usual BCS relation $T_c \simeq 0.567\Delta_F$

Chamel et al., Phys.Rev.C81,045804 (2010).

Neutron pairing gaps vs density

\bar{n} is the average nucleon density

Z is the number of protons in the Wigner-Seitz cell

A is the number of nucleons in the Wigner-Seitz cell

n_n^f is the density of unbound neutrons

Δ_u is the gap in neutron matter at density n_n^f

$\bar{\Delta}_u$ is the gap in neutron matter at density n_n

\bar{n} [fm^{-3}]	Z	A	n_n^f [fm^{-3}]	Δ_F [MeV]	Δ_u [MeV]	$\bar{\Delta}_u$ [MeV]
0.07	40	1218	0.060	1.44	1.79	1.43
0.065	40	1264	0.056	1.65	1.99	1.65
0.06	40	1260	0.051	1.86	2.20	1.87
0.055	40	1254	0.047	2.08	2.40	2.10
0.05	40	1264	0.043	2.29	2.59	2.33

Chamel et al., Phys.Rev.C81,045804 (2010).

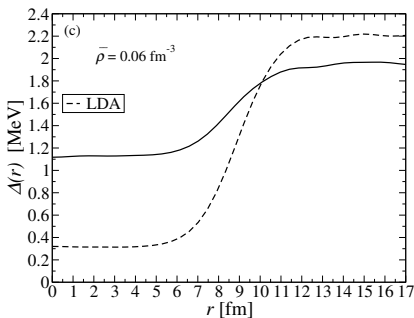
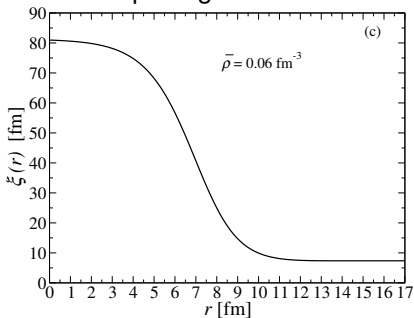
- the nuclear clusters lower the gap by 10 – 20%
- both bound and unbound neutrons contribute to the gap

Pairing field and local density approximation

The effects of inhomogeneities on neutron superfluidity can be directly seen in the pairing field

$$\Delta_n(\mathbf{r}) = -\frac{1}{2} v^{\pi n} [n_n(\mathbf{r}), n_p(\mathbf{r})] \tilde{n}_n(\mathbf{r}), \quad \tilde{n}_n(\mathbf{r}) = \sum_{\alpha, \mathbf{k}}^{\Lambda} |\varphi_{\alpha \mathbf{k}}(\mathbf{r})|^2 \frac{\Delta_{\alpha \mathbf{k}}}{E_{\alpha \mathbf{k}}}$$

Neutron pairing field for $\bar{n} = 0.06 \text{ fm}^{-3}$ at $T = 0$



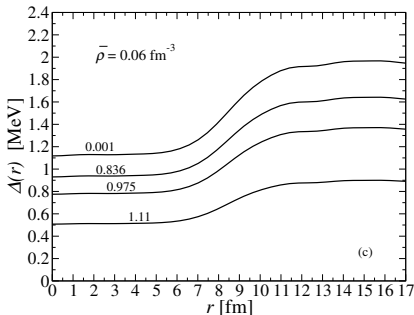
Pairing field at finite temperature

At $T > 0$, the neutron pairing field is given by

$$\Delta_n(\mathbf{r}) = -\frac{1}{2} v^{\pi n} [n_n(\mathbf{r}), n_p(\mathbf{r})] \tilde{n}_n(\mathbf{r}), \quad \tilde{n}_n(\mathbf{r}) = \sum_{\alpha, \mathbf{k}} |\varphi_{\alpha \mathbf{k}}(\mathbf{r})|^2 \frac{\Delta_{\alpha \mathbf{k}}}{E_{\alpha \mathbf{k}}} \tanh \frac{E_{\alpha \mathbf{k}}}{2k_B T}$$

Neutron pairing field for $\bar{n} = 0.06 \text{ fm}^{-3}$

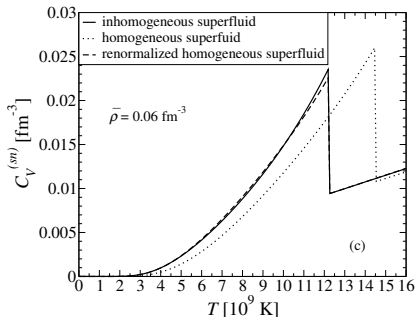
The superfluid becomes more and more homogeneous as T approaches T_c



Chamel et al., *Phys.Rev.C*81(2010)045804.

Impact on thermodynamic quantities : specific heat

Example at $\bar{n} = 0.06 \text{ fm}^{-3}$ with BSk16



- Band structure effects are small. This remains true for non-superfluid neutrons.
Chamel et al, Phys. Rev. C 79, 012801(R) (2009)
- The renormalization of T_c comes from the density dependence of the pairing strength.

Pairing in the shallow layers of neutron-star crusts

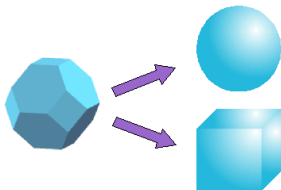
In the shallow layers, the decoupling approximation is not very accurate. On the other hand, solving the full HFB equations is computationally very expensive.

Pairing in the shallow layers of neutron-star crusts

In the shallow layers, the decoupling approximation is not very accurate. On the other hand, solving the full HFB equations is computationally very expensive.

Approximation proposed by Wigner&Seitz in 1933 in the study of metallic sodium (only one valence electron per site):

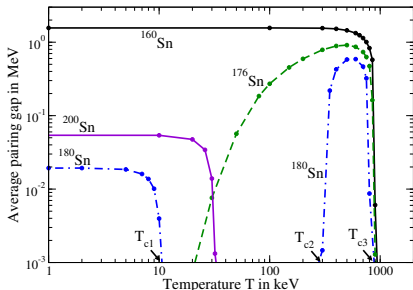
- Consider only $\mathbf{k} = 0$ (i.e. strictly periodic wave functions),
- Replace the W-S cell by a simpler cell of same volume



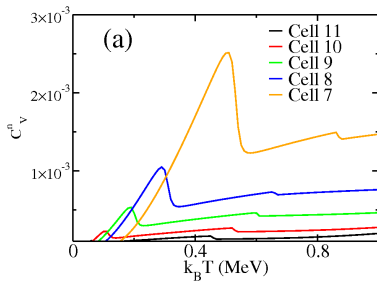
Problem: nonuniqueness of the boundary conditions.

Margueron & Sandulescu, in "Neutron Star Crust" (Nova Science Publisher, 2012).

Pairing in the shallow layers of neutron-star crusts



Margueron&Khan, *PRC86*, 065801(2012).



Pastore, *PRC86*, 065802(2012)

Superfluidity in the crust is very different from neutron matter:

- reentrance phenomenon
- existence of several critical temperatures.

These features cannot be explained by the simple BCS theory.

Superfluids are multi-fluid systems



Tisza and Landau showed that superfluid helium cannot be described using the classical hydrodynamic equations. Two distinct dynamical components coexist:

- a superfluid,
- a normal viscous fluid.

Superfluids are multi-fluid systems



Tisza and Landau showed that superfluid helium cannot be described using the classical hydrodynamic equations. Two distinct dynamical components coexist:

- a superfluid,
- a normal viscous fluid.

In neutron stars, electrically charged particles are locked together by the magnetic field on very long timescales. Neutron stars contain (at least!) **two dynamical components**:

- a plasma of charged particles
- a neutron superfluid.

Baym et al, Nature 224 (1969), 673.

Relativistic multifluid hydrodynamics is required for modelling superfluid neutron stars.

Mutual entrainment

In superfluid mixtures such as ^3He - ^4He , the different superfluid constituents may still be **mutually entrained**:

$$\rho_{\mathbf{X}} = \sum_Y \mathcal{K}^{\mathbf{X}\mathbf{Y}} \mathbf{v}_{\mathbf{Y}} \Leftrightarrow \mathbf{j}_{\mathbf{X}} = \sum_Y \rho_{\mathbf{X}\mathbf{Y}} \mathbf{V}_{\mathbf{Y}}$$

$\rho_{\mathbf{X}}$ is the momentum of the component X

$\mathbf{v}_{\mathbf{Y}}$ is the velocity of the component Y

$\mathbf{j}_{\mathbf{X}}$ is the mass current of the component X

$\mathbf{V}_{\mathbf{Y}} = \frac{\rho_{\mathbf{Y}}}{m_{\mathbf{Y}}}$ is the "superfluid velocity" of the component Y

$\mathcal{K}^{\mathbf{X}\mathbf{Y}}$ and $\rho_{\mathbf{X}\mathbf{Y}}$ are symmetric matrices, which depend on the interactions between the constituent particles.

Andreev & Bashkin, Sov. Phys. JETP 42, 164 (1975).

Mutual entrainment

In superfluid mixtures such as ^3He - ^4He , the different superfluid constituents may still be **mutually entrained**:

$$\rho_{\mathbf{X}} = \sum_{\mathbf{Y}} \mathcal{K}^{\mathbf{XY}} \mathbf{v}_{\mathbf{Y}} \Leftrightarrow \mathbf{j}_{\mathbf{X}} = \sum_{\mathbf{Y}} \rho_{\mathbf{XY}} \mathbf{V}_{\mathbf{Y}}$$

$\rho_{\mathbf{X}}$ is the momentum of the component X

$\mathbf{v}_{\mathbf{Y}}$ is the velocity of the component Y

$\mathbf{j}_{\mathbf{X}}$ is the mass current of the component X

$\mathbf{V}_{\mathbf{Y}} = \frac{\rho_{\mathbf{Y}}}{m_{\mathbf{Y}}}$ is the "superfluid velocity" of the component Y

$\mathcal{K}^{\mathbf{XY}}$ and $\rho_{\mathbf{XY}}$ are symmetric matrices, which depend on the interactions between the constituent particles.

Andreev & Bashkin, Sov. Phys. JETP 42, 164 (1975).

Entrainment is nondissipative and is therefore different from drag since superfluids have no viscosity !

Not all matrix elements are independent. Galilean invariance requires

$$m_{\mathbf{X}} = \sum_{\mathbf{Y}} \mathcal{K}^{\mathbf{XY}} \Leftrightarrow \rho_{\mathbf{X}} = \sum_{\mathbf{Y}} \rho_{\mathbf{XY}}$$

Mutual entrainment in ^3He - ^4He mixtures at $T = 0$

Galilean invariance requires

$$\begin{aligned}m_3 &= \mathcal{K}^{33} + \mathcal{K}^{34} , \\m_4 &= \mathcal{K}^{44} + \mathcal{K}^{43} ,\end{aligned}$$

and since $\mathcal{K}^{34} = \mathcal{K}^{43}$, entrainment is determined by only one matrix element.

Mutual entrainment in ${}^3\text{He}$ - ${}^4\text{He}$ mixtures at $T = 0$

Galilean invariance requires

$$\begin{aligned}m_3 &= \mathcal{K}^{33} + \mathcal{K}^{34} , \\m_4 &= \mathcal{K}^{44} + \mathcal{K}^{43} ,\end{aligned}$$

and since $\mathcal{K}^{34} = \mathcal{K}^{43}$, entrainment is determined by only one matrix element.

Entrainment can be expressed in terms of "**effective masses**", but different definitions are possible:

Mutual entrainment in ${}^3\text{He}$ - ${}^4\text{He}$ mixtures at $T = 0$

Galilean invariance requires

$$\begin{aligned}m_3 &= \mathcal{K}^{33} + \mathcal{K}^{34} , \\m_4 &= \mathcal{K}^{44} + \mathcal{K}^{43} ,\end{aligned}$$

and since $\mathcal{K}^{34} = \mathcal{K}^{43}$, entrainment is determined by only one matrix element.

Entrainment can be expressed in terms of "**effective masses**", but different definitions are possible:

- $\mathbf{v}_3 = 0 \Rightarrow \rho_4 = m_4^* \mathbf{v}_4$ with $m_4^* = \mathcal{K}^{44}$ and vice versa

Mutual entrainment in ${}^3\text{He}$ - ${}^4\text{He}$ mixtures at $T = 0$

Galilean invariance requires

$$\begin{aligned}m_3 &= \mathcal{K}^{33} + \mathcal{K}^{34} , \\m_4 &= \mathcal{K}^{44} + \mathcal{K}^{43} ,\end{aligned}$$

and since $\mathcal{K}^{34} = \mathcal{K}^{43}$, entrainment is determined by only one matrix element.

Entrainment can be expressed in terms of "**effective masses**", but different definitions are possible:

- $\mathbf{v}_3 = 0 \Rightarrow \mathbf{p}_4 = m_4^* \mathbf{v}_4$ with $m_4^* = \mathcal{K}^{44}$ and vice versa
- $\mathbf{p}_3 = 0 \Rightarrow \mathbf{p}_4 = m_4^\# \mathbf{v}_4$ with $m_4^\# = \mathcal{K}^{44} - \frac{\mathcal{K}^{43}\mathcal{K}^{34}}{\mathcal{K}^{33}} \neq m_4^*$ and vice versa.

Mutual entrainment in ${}^3\text{He}$ - ${}^4\text{He}$ mixtures at $T = 0$

Galilean invariance requires

$$\begin{aligned}m_3 &= \mathcal{K}^{33} + \mathcal{K}^{34} , \\m_4 &= \mathcal{K}^{44} + \mathcal{K}^{43} ,\end{aligned}$$

and since $\mathcal{K}^{34} = \mathcal{K}^{43}$, entrainment is determined by only one matrix element.

Entrainment can be expressed in terms of "**effective masses**", but different definitions are possible:

- $\mathbf{v}_3 = 0 \Rightarrow \mathbf{p}_4 = m_4^* \mathbf{v}_4$ with $m_4^* = \mathcal{K}^{44}$ and vice versa
- $\mathbf{p}_3 = 0 \Rightarrow \mathbf{p}_4 = m_4^\# \mathbf{v}_4$ with $m_4^\# = \mathcal{K}^{44} - \frac{\mathcal{K}^{43}\mathcal{K}^{34}}{\mathcal{K}^{33}} \neq m_4^*$ and vice versa.

Generalized equations of state are needed for modelling superfluid neutron stars.

How to obtain flow equations for (super)fluid mixtures?

Generalizing Tisza-Landau's nonrelativistic two-fluid model of superfluid helium to arbitrary relativistic superfluid mixtures is not straightforward.

How to obtain flow equations for (super)fluid mixtures?

Generalizing Tisza-Landau's nonrelativistic two-fluid model of superfluid helium to arbitrary relativistic superfluid mixtures is not straightforward.



An elegant variational formalism was developed by Brandon Carter using exterior calculus.

Carter in "Relativistic fluid dynamics" (Springer-Verlag, 1989), pp.1-64

Carter, Lect. Notes Phys. 578 (2001), Springer

Andersson&Comer, Living Rev. Relativity 10 (2007), 1.

How to obtain flow equations for (super)fluid mixtures?

Generalizing Tisza-Landau's nonrelativistic two-fluid model of superfluid helium to arbitrary relativistic superfluid mixtures is not straightforward.



An elegant variational formalism was developed by Brandon Carter using exterior calculus.

Carter in "Relativistic fluid dynamics" (Springer-Verlag, 1989), pp.1-64

Carter, Lect. Notes Phys. 578 (2001), Springer

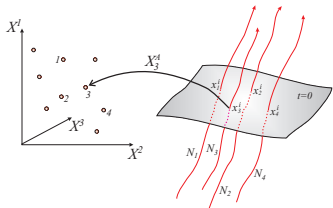
Andersson&Comer, Living Rev. Relativity 10 (2007), 1.

This formalism relies on an **action integral** $\mathcal{A} = \int \Lambda\{n_x^\mu\} d\mathcal{M}^{(4)}$ over the 4-dimensional manifold $\mathcal{M}^{(4)}$ (Newtonian or Riemannian).

The Lagrangian density or **master function** Λ depends on the 4-current vectors $n_x^\mu = n_x u_x^\mu$ of the different fluids X.

For a short pedagogical introduction, see e.g. *Gourgoulhon, EAS Publications Series 21 (2006), 43.*

Variational formulation of superfluid hydrodynamics



picture from Andersson&Comer

Using the action principle and considering variations of the fluid particle trajectories yield

$$n_X^\mu \varpi_{\mu\nu}^X + \pi_\nu^X \nabla_\mu n_X^\mu = f_\nu^X$$

4-momentum covector

$$\pi_\mu^X = \frac{\partial \Lambda}{\partial n_X^\mu}$$

vorticity 2-form

$$\varpi_{\mu\nu}^X = 2\nabla_{[\mu} \pi_{\nu]}^X = \nabla_\mu \pi_\nu^X - \nabla_\nu \pi_\mu^X$$

4-force density covector

$$f_\nu^X$$

Remark: π_μ^X and n_X^μ are mathematically different objects: the first is a *covector*, while the second is a *vector*. This distinction is fundamental in Newtonian spacetime (no metric).

Stress-energy density tensor and generalized pressure

Using Noether identities leads to the stress-energy density tensor of the superfluid mixture

$$T_{\nu}^{\mu} = \Psi \delta_{\nu}^{\mu} + \sum_x n_x^{\mu} \pi_{\nu}^x$$

where Ψ is a **generalized pressure**

$$\Psi = \Lambda - \sum_x n_x^{\mu} \pi_{\mu}^x.$$

In general, Ψ depends on the velocities of the fluids.

The above expressions are valid for any spacetime.

Example: cold relativistic superfluid

Let us consider a single relativistic superfluid at $T = 0$. The master function is simply $\Lambda = -\rho c^2$, where ρ is the mass-energy density.

Example: cold relativistic superfluid

Let us consider a single relativistic superfluid at $T = 0$. The master function is simply $\Lambda = -\rho c^2$, where ρ is the mass-energy density.

The 4-current is $n^\mu = n u^\mu$, where n is the particle number density and u^μ the 4-velocity, normalized as $u^\mu u_\mu = -c^2$.

Example: cold relativistic superfluid

Let us consider a single relativistic superfluid at $T = 0$. The master function is simply $\Lambda = -\rho c^2$, where ρ is the mass-energy density.

The 4-current is $n^\mu = n u^\mu$, where n is the particle number density and u^μ the 4-velocity, normalized as $u^\mu u_\mu = -c^2$.

The variation of the master function can be expressed as

$$\delta\Lambda = -\mu\delta n = \frac{\mu}{c^2} u_\nu \delta n^\nu$$

where μ is the chemical potential.

Example: cold relativistic superfluid

Let us consider a single relativistic superfluid at $T = 0$. The master function is simply $\Lambda = -\rho c^2$, where ρ is the mass-energy density.

The 4-current is $n^\mu = n u^\mu$, where n is the particle number density and u^μ the 4-velocity, normalized as $u^\mu u_\mu = -c^2$.

The variation of the master function can be expressed as

$$\delta\Lambda = -\mu\delta n = \frac{\mu}{c^2} u_\nu \delta n^\nu$$

where μ is the chemical potential.

The 4-momentum is thus given by $\pi_\nu = \frac{\partial\Lambda}{\partial n^\nu} = \frac{\mu}{c^2} u_\nu$.

Example: cold relativistic superfluid

Let us consider a single relativistic superfluid at $T = 0$. The master function is simply $\Lambda = -\rho c^2$, where ρ is the mass-energy density.

The 4-current is $n^\mu = n u^\mu$, where n is the particle number density and u^μ the 4-velocity, normalized as $u^\mu u_\mu = -c^2$.

The variation of the master function can be expressed as

$$\delta\Lambda = -\mu\delta n = \frac{\mu}{c^2} u_\nu \delta n^\nu$$

where μ is the chemical potential.

The 4-momentum is thus given by $\pi_\nu = \frac{\partial\Lambda}{\partial n^\nu} = \frac{\mu}{c^2} u_\nu$.

The generalized pressure reduces to the ordinary pressure

$$\Psi \equiv \Lambda - n^\mu \pi_\mu = -\rho c^2 + n\mu = P.$$

Example: cold relativistic superfluid

Let us consider a single relativistic superfluid at $T = 0$. The master function is simply $\Lambda = -\rho c^2$, where ρ is the mass-energy density.

The 4-current is $n^\mu = n u^\mu$, where n is the particle number density and u^μ the 4-velocity, normalized as $u^\mu u_\mu = -c^2$.

The variation of the master function can be expressed as

$$\delta\Lambda = -\mu\delta n = \frac{\mu}{c^2} u_\nu \delta n^\nu$$

where μ is the chemical potential.

The 4-momentum is thus given by $\pi_\nu = \frac{\partial\Lambda}{\partial n^\nu} = \frac{\mu}{c^2} u_\nu$.

The generalized pressure reduces to the ordinary pressure

$$\Psi \equiv \Lambda - n^\mu \pi_\mu = -\rho c^2 + n\mu = P.$$

Using the relation $P = n\mu - \rho c^2$, the stress-energy density tensor is

$$T_\nu^\mu \equiv \Psi \delta_\nu^\mu + n^\mu \pi_\nu = P\delta_\nu^\mu + \left(\rho + \frac{P}{c^2}\right) u^\mu u_\nu.$$

Superfluidity vs perfect fluidity

In a rotating superfluid, the circulation $\oint \pi_{\mu}^x dx^{\mu} = Nh$ is quantized into N vortices. Let d_v be the intervortex spacing.

Superfluidity vs perfect fluidity

In a rotating superfluid, the circulation $\oint \pi_{\mu}^x dx^{\mu} = Nh$ is quantized into N vortices. Let d_v be the intervortex spacing.

- On a scale $\ell \ll d_v$: the superfluid is irrotational

$$\varpi_{\mu\nu}^x = 0 \Rightarrow \pi_{\mu}^x = \hbar \nabla_{\mu} \phi^x$$

where ϕ^x is the quantum phase of the (boson) condensate.

Superfluidity vs perfect fluidity

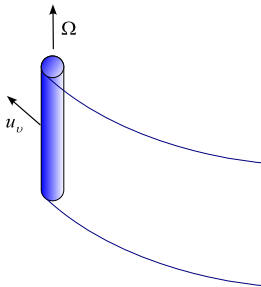
In a rotating superfluid, the circulation $\oint \pi_\mu^x dx^\mu = Nh$ is quantized into N vortices. Let d_v be the intervortex spacing.

- On a scale $\ell \ll d_v$: the superfluid is irrotational

$$\varpi_{\mu\nu}^x = 0 \Rightarrow \pi_\mu^x = \hbar \nabla_\mu \phi^x$$

where ϕ^x is the quantum phase of the (boson) condensate.

- On a scale $\ell \gg d_v$: the superfluid rotates as a rigid body



vorticity is carried along u_v^μ

$$\vec{u}_v \mathcal{L} \varpi_{\mu\nu}^x = 0$$

$$\Rightarrow u_v^\mu \varpi_{\mu\nu}^x = 0$$

Relativistic two-fluid models of neutron stars

The simplest model of cold superfluid neutron star cores contains two components:

- a “proton” fluid
- a neutron superfluid.

Relativistic two-fluid models of neutron stars

The simplest model of cold superfluid neutron star cores contains two components:

- a “proton” fluid
- a neutron superfluid.

The corresponding master function can be expressed as

$$\Lambda = -\rho(n_n, n_p)c^2 + \lambda_1(n_n, n_p)(x^2 - n_n n_p) + \lambda_2(n_n, n_p)(x^2 - n_n n_p)^2 + \dots$$

$$\text{with } x^2 c^2 = -g_{\mu\nu} n_n^\mu n_p^\nu, \quad n_n^2 c^2 = -g_{\mu\nu} n_n^\mu n_n^\nu, \quad n_p^2 c^2 = -g_{\mu\nu} n_p^\mu n_p^\nu.$$

Relativistic two-fluid models of neutron stars

The simplest model of cold superfluid neutron star cores contains two components:

- a “proton” fluid
- a neutron superfluid.

The corresponding master function can be expressed as

$$\Lambda = -\rho(n_n, n_p)c^2 + \lambda_1(n_n, n_p)(x^2 - n_n n_p) + \lambda_2(n_n, n_p)(x^2 - n_n n_p)^2 + \dots$$

$$\text{with } x^2 c^2 = -g_{\mu\nu} n_n^\mu n_p^\nu, \quad n_n^2 c^2 = -g_{\mu\nu} n_n^\mu n_n^\nu, \quad n_p^2 c^2 = -g_{\mu\nu} n_p^\mu n_p^\nu.$$

The gravitational field is described by the Einstein-Hilbert Lagrangian

$$\text{density } \Lambda_{\text{EH}} = \frac{c^4}{16\pi G} R, \text{ where } R \text{ is the Ricci scalar.}$$

Relativistic two-fluid models of neutron stars

The simplest model of cold superfluid neutron star cores contains two components:

- a “proton” fluid
- a neutron superfluid.

The corresponding master function can be expressed as

$$\Lambda = -\rho(n_n, n_p)c^2 + \lambda_1(n_n, n_p)(x^2 - n_n n_p) + \lambda_2(n_n, n_p)(x^2 - n_n n_p)^2 + \dots$$

$$\text{with } x^2 c^2 = -g_{\mu\nu} n_n^\mu n_p^\nu, \quad n_n^2 c^2 = -g_{\mu\nu} n_n^\mu n_n^\nu, \quad n_p^2 c^2 = -g_{\mu\nu} n_p^\mu n_p^\nu.$$

The gravitational field is described by the Einstein-Hilbert Lagrangian density $\Lambda_{\text{EH}} = \frac{c^4}{16\pi G} R$, where R is the Ricci scalar.

The microscopic physics is embedded in the usual equation of state $\rho(n_n, n_p)$, and in the entrainment coefficients $\lambda_1(n_n, n_p)$, $\lambda_2(n_n, n_p) \dots$

Microscopic calculations of $\lambda_1(n_n, n_p)$:

- (non)relativistic Fermi liquid theory,
- (non)relativistic “mean field” theory.

Relativistic models of superfluid neutron stars

The simple two-fluid model can be easily extended to account for the neutron superfluid permeating the inner crust.

Carter, Chamel, Haensel, Int. J. Mod. Phys. D15, 777 (2006)

Relativistic models of superfluid neutron stars

The simple two-fluid model can be easily extended to account for the neutron superfluid permeating the inner crust.

Carter, Chamel, Haensel, Int. J. Mod. Phys. D15, 777 (2006)

Despite the absence of viscous drag, the crust can still be entrained by the superfluid due to Bragg scattering: $\lambda_1(n_n, n_p)$, $\lambda_2(n_n, n_p) \dots$ do not vanish in the inner crust.

Chamel, PhD thesis, Université Paris 6, France (2004)

Carter, Chamel, Haensel, Nucl. Phys. A748, 675 (2005)

Relativistic models of superfluid neutron stars

The simple two-fluid model can be easily extended to account for the neutron superfluid permeating the inner crust.

Carter, Chamel, Haensel, Int. J. Mod. Phys. D15, 777 (2006)

Despite the absence of viscous drag, the crust can still be entrained by the superfluid due to Bragg scattering: $\lambda_1(n_n, n_p)$, $\lambda_2(n_n, n_p) \dots$ do not vanish in the inner crust.

Chamel, PhD thesis, Université Paris 6, France (2004)

Carter, Chamel, Haensel, Nucl. Phys. A748, 675 (2005)

The presence of a magnetic field and elasticity can be also included:

- non-relativistic formulation

Carter, Chachoua & Chamel, Gen. Rel. Grav. 38, 83 (2006).

Carter & Chachoua, Int. J. Mod. Phys. D15, 1329 (2006).

Pethick, Chamel & Reddy, Prog. Theo. Phys. Sup. 186, 9 (2010).

Andersson, Haskell, Samuelsson, MNRAS 416, 118 (2011).

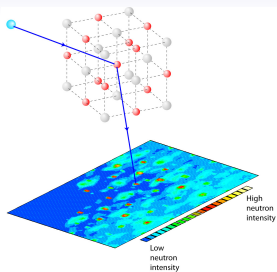
- relativistic formulation

Carter & Samuelsson, Class. Quant. Grav. 23, 5367 (2006).

Bragg scattering

For decades, neutron diffraction experiments have been routinely performed to explore the structure of materials.

The main difference in neutron-star crusts is that **neutrons are highly degenerate**



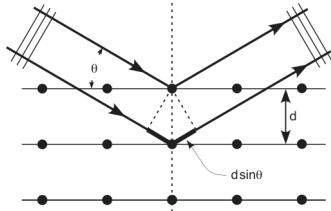
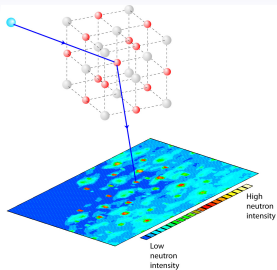
Bragg scattering

For decades, neutron diffraction experiments have been routinely performed to explore the structure of materials.

The main difference in neutron-star crusts is that **neutrons are highly degenerate**

A neutron with wavevector \mathbf{k} can be **coherently scattered** if $d \sin \theta = N\pi/k$, where $N = 0, 1, 2, \dots$ (Bragg's law).

In this case, it does not propagate in the crystal: it is therefore entrained!



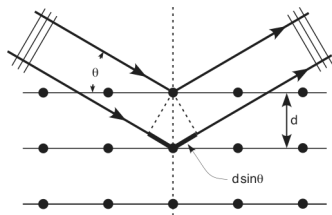
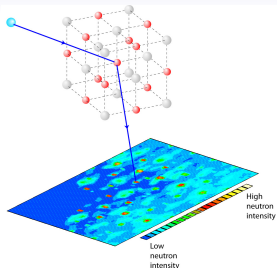
Bragg scattering

For decades, neutron diffraction experiments have been routinely performed to explore the structure of materials.

The main difference in neutron-star crusts is that **neutrons are highly degenerate**

A neutron with wavevector \mathbf{k} can be **coherently scattered** if $d \sin \theta = N\pi/k$, where $N = 0, 1, 2, \dots$ (Bragg's law).

In this case, it does not propagate in the crystal: it is therefore entrained!

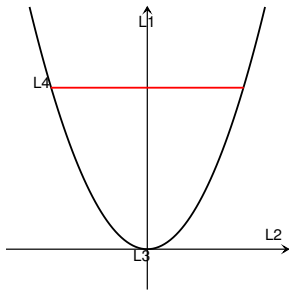


Bragg scattering occurs if $k > \pi/d$. In neutron stars, neutrons have momenta up to k_F . Typically $k_F > \pi/d$ in all regions of the inner crust but the shallowest.

Neutron conduction: free neutrons

ground state

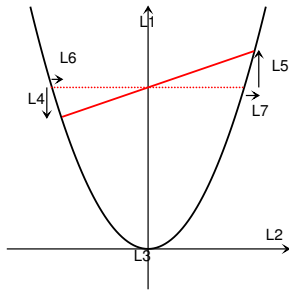
$$\varepsilon_{\mathbf{k}} < \mu$$



$$\mathbf{j}_n = 0$$

conducting state

$$\varepsilon_{\mathbf{k}} < \mu + \mathbf{p}_n \cdot \nabla_{\mathbf{k}} \varepsilon_{\mathbf{k}}$$



$$\mathbf{j}_n = n_n^f \mathbf{p}_n \text{ with } \mathbf{p}_n = \hbar \delta \mathbf{k}$$

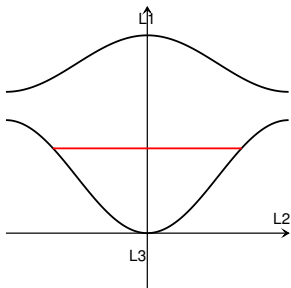
Define an **effective mass** $m_n^* = m_n \frac{n_n^f}{n_n^c}$ such that $\mathbf{p}_n \equiv m_n^* \mathbf{v}_n$, where \mathbf{v}_n is the average neutron velocity defined by $\mathbf{j}_n = n_n^f m_n \mathbf{v}_n$.

All free neutrons contribute to the current: $m_n^* = m_n$

Neutron conduction: neutrons in a periodic potential

ground state

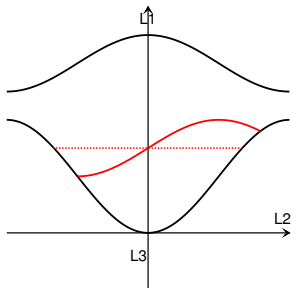
$$\varepsilon_{\alpha\mathbf{k}} < \mu$$



$$\mathbf{j}_n = 0$$

conducting state

$$\varepsilon_{\alpha\mathbf{k}} < \mu + \mathbf{p}_n \cdot \nabla_{\mathbf{k}} \varepsilon_{\alpha\mathbf{k}}$$



$$\mathbf{j}_n = n_n^c \mathbf{p}_n$$

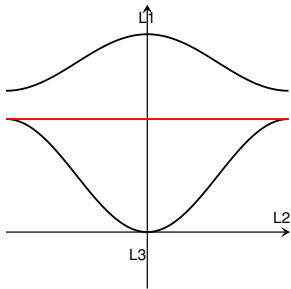
Only some “conduction” neutrons contribute to the current:

$$n_n^c = \frac{m_n}{24\pi^3 \hbar^2} \sum_{\alpha} \int_{\mathcal{F}} |\nabla_{\mathbf{k}} \varepsilon_{\alpha\mathbf{k}}| dS^{(\alpha)} \leq n_n^f \Rightarrow m_n^* \geq m_n$$

Neutron conduction: neutrons in a periodic potential

ground state

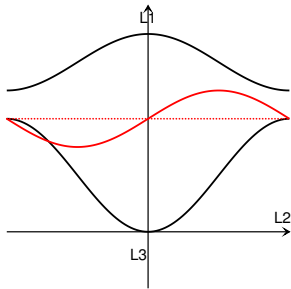
$$\varepsilon_{\alpha k} < \mu$$



$$\mathbf{j}_n = 0$$

conducting state

$$\varepsilon_{\alpha k} < \mu + \mathbf{p}_n \cdot \nabla_k \varepsilon_{\alpha k}$$



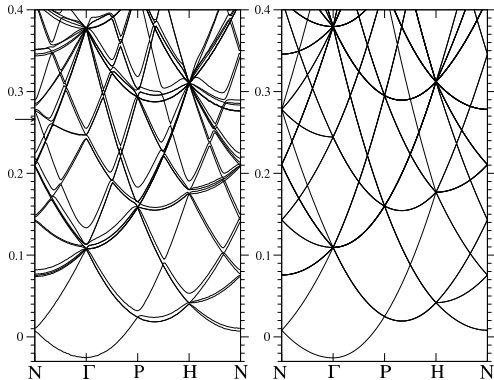
$$\mathbf{j}_n = n_n^c \mathbf{p}_n = 0 \text{ but } \mathbf{p}_n \neq 0$$

If the Fermi level lies in a gap, no current can flow since there is no available states! All neutrons are therefore entrained:

$$n_n^c = 0 \Leftrightarrow m_n^* \rightarrow +\infty$$

Neutron band structure: shallow region

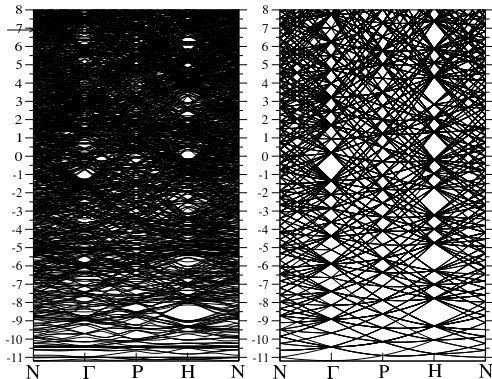
Neutron band structure (s.p. energy in MeV vs \mathbf{k}) with (left) and without (right) a bcc lattice of tin like clusters:



The band structure is similar to that of free neutrons: entrainment is therefore expected to be weak.

Neutron band structure: intermediate region

Neutron band structure (s.p. energy in MeV vs \mathbf{k}) with (left) and without (right) a bcc lattice of zirconium like clusters:



The band structure is very different from that of free neutrons: entrainment is therefore expected to be strong.

How “free” are neutrons in neutron-star crusts?

Results of systematic band structure calculations in all regions of the inner crust of a neutron star using accurately calibrated Skyrme nuclear energy density functional BSk14:

\bar{n} (fm^{-3})	n_n^f/n_n (%)	n_n^c/n_n^f (%)
0.0003	20.0	82.6
0.001	68.6	27.3
0.005	86.4	17.5
0.01	88.9	15.5
0.02	90.3	7.37
0.03	91.4	7.33
0.04	88.8	10.6
0.05	91.4	30.0
0.06	91.5	45.9

\bar{n} is the average baryon density

n_n is the total neutron density

n_n^f is the “free” neutron density

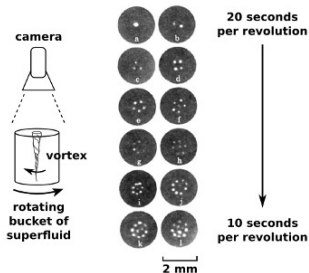
n_n^c is the “conduction” neutron density

In many layers, most neutrons are entrained by the crust!

Chamel, PRC85, 035801 (2012)

Superfluid vortices

A rotating superfluid is threaded by **quantized vortex lines**, each of which carries an angular momentum \hbar . The surface density of vortices is given by $n_V(\text{km}^{-2}) \sim 10^{14}/P(\text{s})$.



Yarmchuk, Gordon, and Packard, PRL43, 214 (1979).

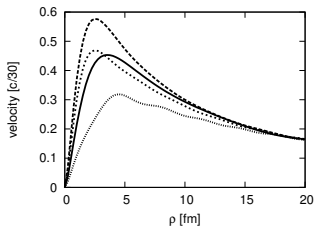
Likewise a type II superconductor is threaded by **flux tubes**.

In a neutron star, the surface density of (proton) flux tubes is expected to be typically $\sim 10^{13} - 10^{14}$ times larger than that of (neutron) vortices. But type I superconductivity is not excluded. *Sedrakian & Clark, in "Pairing in Fermionic Systems", (World Scientific, 2006)*

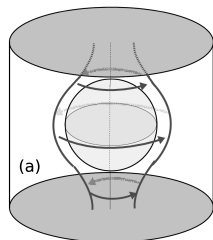
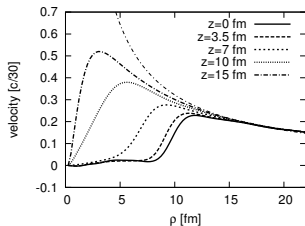
Superfluid vortices in neutron star crust

Neutron superfluid vortices can pin to clusters.

single vortex



single vortex + cluster



Avogadro et al, Nucl.Phys.A811,378(2008).

Microscopic calculations of pinning forces:

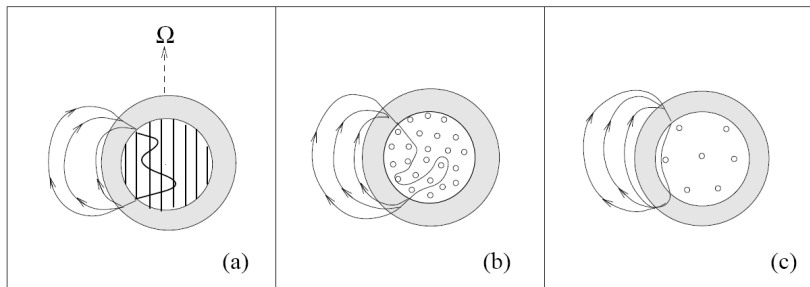
- local density approximation
- semi-classical methods
- self-consistent “mean-field” methods

The actual pinning of vortices depends also on the structure of the crust, on the rigidity of the lines and on the vortex dynamics.

Bulgac, Forbes, Sharma, PRL110, 241102 (2013)

Superfluid vortices in neutron star core

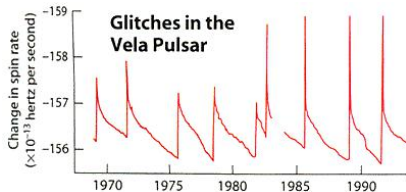
Neutron superfluid vortices can also pin to flux tubes provided the superconductor is of type II. The strong interaction between neutron superfluid vortices and proton flux tubes in neutron star cores leads to movement of crustal plates.



The evolution of the pulsar spin and magnetic field are intimately related to superfluidity and superconductivity

Pulsar glitches

The strongest evidence for nuclear superfluidity come from pulsar **sudden spin-ups**. Similar phenomena were observed in He II.

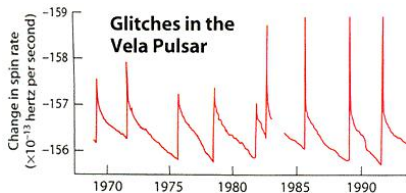


So far 470 glitches have been detected in 165 pulsars.

<http://www.jb.man.ac.uk/pulsar/glitches/gTable.html>

Pulsar glitches

The strongest evidence for nuclear superfluidity come from pulsar **sudden spin-ups**. Similar phenomena were observed in He II.



So far 470 glitches have been detected in 165 pulsars.

<http://www.jb.man.ac.uk/pulsar/glitches/gTable.html>

Vortex pinning by nuclei gives rise to crustal stress until:

- vortices are suddenly unpinned (Anderson&Itoh)
- the crust cracks (Ruderman).

Post-glitch relaxation arises from vortex creep.

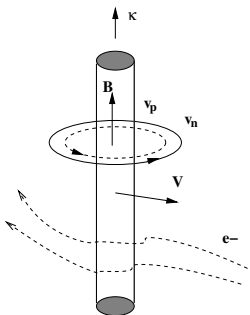
Pines & Alpar, Nature 316, 27(1985)

Entrainment and dissipation in neutron-star cores

Historically the **long post-glitch relaxation** provided the first indications of neutron-star superfluidity. But...

Entrainment and dissipation in neutron-star cores

Historically the **long post-glitch relaxation** provided the first indications of neutron-star superfluidity. But...



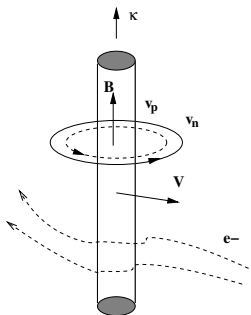
picture from K. Glampedakis

Due to (non-dissipative) mutual entrainment effects, neutron vortices carry a **fractional magnetic quantum flux**

Sedrakyan & Shakhbasyan, Astrofizika 8 (1972), 557; Astrofizika 16 (1980), 727.

Entrainment and dissipation in neutron-star cores

Historically the **long post-glitch relaxation** provided the first indications of neutron-star superfluidity. But...



Due to (non-dissipative) mutual entrainment effects, neutron vortices carry a **fractional magnetic quantum flux**

Sedrakyan & Shakhbasyan, Astrofizika 8 (1972), 557; Astrofizika 16 (1980), 727.

picture from K. Glampedakis

The core superfluid is strongly coupled to the crust due to electrons scattering off the magnetic field of the vortex lines.

Alpar, Langer, Sauls, ApJ282 (1984) 533

Glitches are therefore expected to originate from the crust.

Vela pulsar glitches and crustal entrainment

Vela pulsar glitches are usually interpreted as **sudden transfers of angular momentum between the crustal superfluid and the rest of star.**

Vela pulsar glitches and crustal entrainment

Vela pulsar glitches are usually interpreted as **sudden transfers of angular momentum between the crustal superfluid and the rest of star.**

However this superfluid is also entrained ! Its angular momentum can thus be written as

$$J_s = I_{ss}\Omega_s + (I_s - I_{ss})\Omega_c$$

(Ω_s and Ω_c being the angular velocities of the superfluid and the “crust”),

Vela pulsar glitches and crustal entrainment

Vela pulsar glitches are usually interpreted as **sudden transfers of angular momentum between the crustal superfluid and the rest of star.**

However this superfluid is also entrained ! Its angular momentum can thus be written as

$$J_s = I_{ss}\Omega_s + (I_s - I_{ss})\Omega_c$$

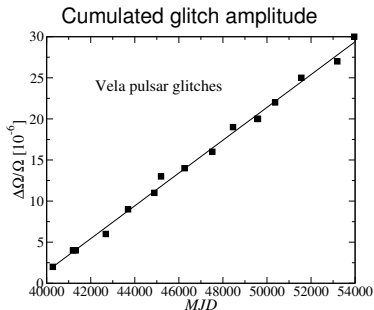
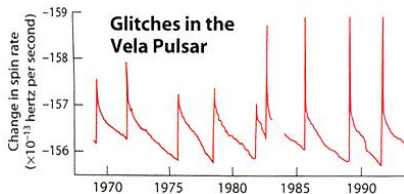
(Ω_s and Ω_c being the angular velocities of the superfluid and the “crust”), leading to the following constraint:

$$\frac{(I_s)^2}{I_{ss}I} \geq A_g \frac{\Omega}{|\dot{\Omega}|}, \quad A_g = \frac{1}{t} \sum_i \frac{\Delta\Omega_i}{\Omega}$$

Chamel&Carter, MNRAS368,796(2006)

Pulsar glitch constraint

Since 1969, 17 glitches have been regularly detected. The latest one occurred in August 2010.



A linear fit of $\frac{\Delta\Omega}{\Omega}$ vs t yields

$$A_g \simeq 2.25 \times 10^{-14} \text{ s}^{-1}$$

$$\frac{(I_s)^2}{I_{ss} I} \geq 1.6\%$$

Moments of inertia

The ratio $(I_s)^2/I_{ss}I$ depends on the internal structure of the star:

$$\frac{(I_s)^2}{I_{ss}} = \frac{I_{\text{crust}}}{I_{ss}} \left(\frac{I_s}{I_{\text{crust}}} \right)^2 \frac{I_{\text{crust}}}{I}.$$

I_{ss}/I_{crust} and I_s/I_{crust} depend only on the crust physics:

$$\frac{I_{ss}}{I_{\text{crust}}} \approx \frac{1}{P_{cc}} \int_{P_{\text{drip}}}^{P_{cc}} \frac{n_n^f(P)^2}{\bar{n}(P)n_n^c(P)} dP, \quad \frac{I_s}{I_{\text{crust}}} \approx \frac{1}{P_{\text{core}}} \int_{P_{\text{drip}}}^{P_{cc}} \frac{n_n^f(P)}{\bar{n}(P)} dP.$$

Moments of inertia

The ratio $(I_s)^2/I_{ss}I$ depends on the internal structure of the star:

$$\frac{(I_s)^2}{I_{ss}} = \frac{I_{\text{crust}}}{I_{ss}} \left(\frac{I_s}{I_{\text{crust}}} \right)^2 \frac{I_{\text{crust}}}{I}.$$

I_{ss}/I_{crust} and I_s/I_{crust} depend only on the crust physics:

$$\frac{I_{ss}}{I_{\text{crust}}} \approx \frac{1}{P_{cc}} \int_{P_{\text{drip}}}^{P_{cc}} \frac{n_n^f(P)^2}{\bar{n}(P)n_n^c(P)} dP, \quad \frac{I_s}{I_{\text{crust}}} \approx \frac{1}{P_{\text{core}}} \int_{P_{\text{drip}}}^{P_{cc}} \frac{n_n^f(P)}{\bar{n}(P)} dP.$$

Using our crust model, we find $I_{ss} \simeq 4.6I_{\text{crust}}$ and $I_s \simeq 0.89I_{\text{crust}}$ leading to $(I_s)^2/I_{ss} \simeq 0.17I_{\text{crust}}$.

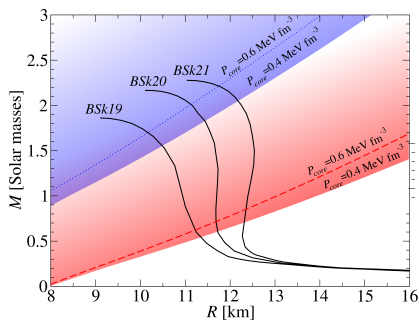
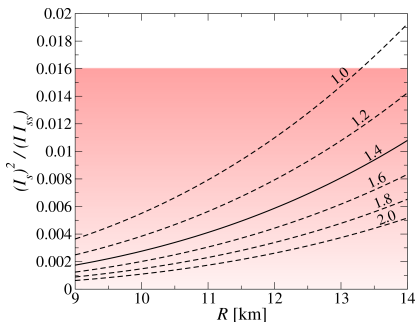
The ratio I_{crust}/I depends on the global structure of the star (M, R) and the crust-core transition (n_{cc}, P_{cc}).

The pulsar glitch constraint thus becomes $\frac{I_{\text{crust}}}{I} \geq 9.4\%$.

Chamel, PRL 110, 011101 (2013).

Pulsar glitch constraint

Shaded areas are excluded if Vela pulsar glitches originate in the crust (Lattimer&Prakash interpolation formula was used):



The inferred mass of Vela is unrealistically low $M < M_{\odot}$.

The crust does not carry enough angular momentum.

Andersson et al. PRL 109, 241103; Chamel, PRL 110, 011101.

Core-induced glitches (pinning to flux tubes)?

Gügercinoğlu & Alpar, ApJ 788, L11 (2014).

Puzzling glitches

The glitch theory has been challenged by other observations:

- a huge glitch in PSR 2334+61
Alpar, AIP Conf.Proc.1379,166(2011)
- unusual post-glitch relaxation in PSR J1119–6127
Weltevrede et al., MNRAS 411,1917(2011)
- a huge glitch in PSR J1718–3718
Manchester & Hobbs, ApJ 736,L31(2011)
- an anti-glitch in 1E 2259+586
Archibald et al.,Nature 497,591 (2013).

Puzzling glitches

The glitch theory has been challenged by other observations:

- a huge glitch in PSR 2334+61
Alpar, AIP Conf.Proc.1379,166(2011)
- unusual post-glitch relaxation in PSR J1119–6127
Weltevrede et al., MNRAS 411,1917(2011)
- a huge glitch in PSR J1718–3718
Manchester & Hobbs, ApJ 736,L31(2011)
- an anti-glitch in 1E 2259+586
Archibald et al.,Nature 497,591 (2013).

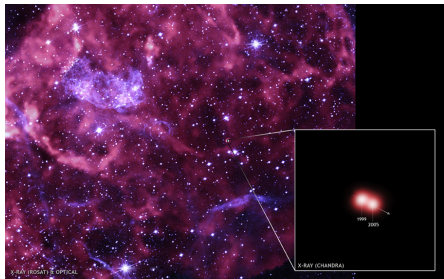
Several physical aspects are not well-understood:

- type of superconductivity
- vortex pinning
- superfluid turbulence
- entrainment
- crust-core coupling.

Haskell&Melatos, Int. J. Mod. Phys. D 24, 1530008 (2015).

Cooling of isolated neutron stars

During the first tens of seconds, the newly formed proto-neutron star with a radius of ~ 50 km stays very hot with $T \sim 10^{11} - 10^{12}$ K. Within $\sim 10 - 20$ s the proto-neutron star becomes transparent to neutrinos and thus rapidly cools down by powerful **neutrino emission** shrinking into an ordinary neutron star.

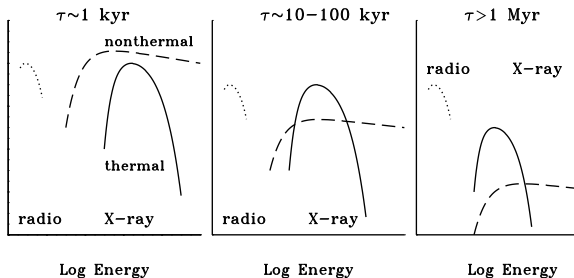


Puppis A (RX J0822-4300) from Chandra

After about $10^4 - 10^5$ years, the cooling is governed by the **emission of thermal photons** due to the diffusion of heat from the interior to the surface.

Thermal X-ray emission of neutron stars

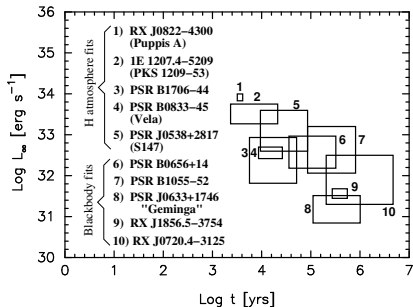
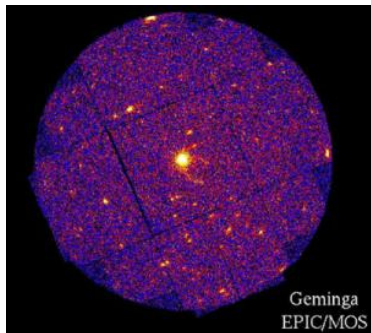
- The thermal X-ray emission of young neutron stars is usually hindered by the magnetospheric component.
- For old pulsars, the thermal radiation dominates but is too low to be detectable (except for hot polar caps).



Picture from Zavlin

Thermal X-ray emission of neutron stars

The best targets are isolated mature neutron stars with no magnetospheric activity: Compact Central Objects (CCOs), Dim Isolated Neutron Stars (DINS).



Page and Reddy, *Ann.Rev.Nucl.Part.Sys.* 56 (2006), 327.

<http://www.astroscu.unam.mx/neutrones/home.html>

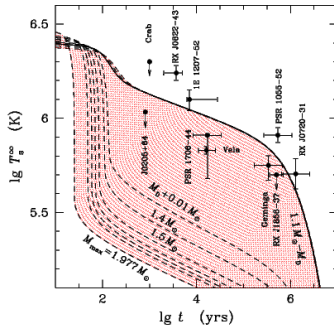
Cooling of neutron stars

Theoretical cooling simulations yield the surface temperature vs age. The curve depends on neutron star mass, radius, composition, presence of magnetic field and superfluidity.

Cooling of neutron stars

Theoretical cooling simulations yield the surface temperature vs age. The curve depends on neutron star mass, radius, composition, presence of magnetic field and superfluidity.

no superfluidity

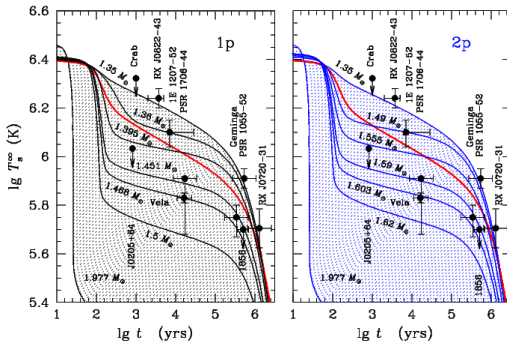


Yakovlev and Pethick, Ann.Rev.Astron.Astrophys 42 (2004), 169

Cooling of neutron stars

Theoretical cooling simulations yield the surface temperature vs age. The curve depends on neutron star mass, radius, composition, presence of magnetic field and superfluidity.

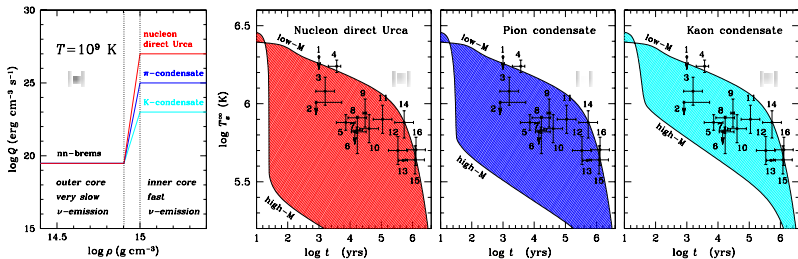
proton superfluidity



Cooling of neutron stars

Theoretical cooling simulations yield the surface temperature vs age. The curve depends on neutron star mass, radius, composition, presence of magnetic field and superfluidity.

exotica

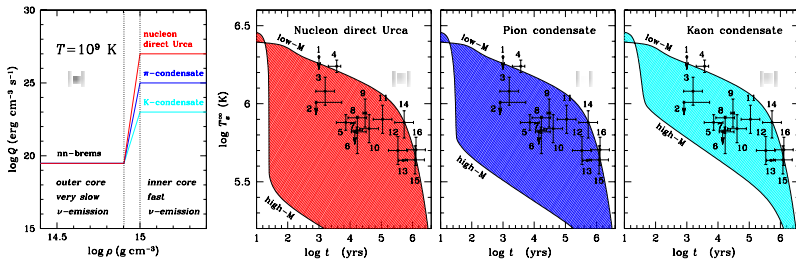


Yakovlev et al, proceedings (2007), arXiv:0710.2047

Cooling of neutron stars

Theoretical cooling simulations yield the surface temperature vs age. The curve depends on neutron star mass, radius, composition, presence of magnetic field and superfluidity.

exotica



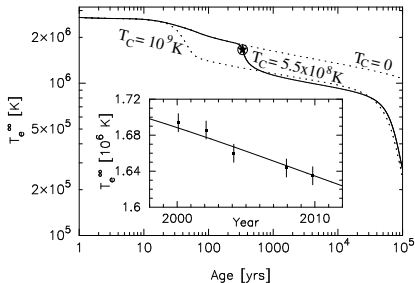
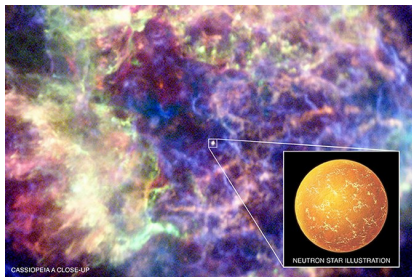
Yakovlev et al, proceedings (2007), arXiv:0710.2047

The thermal X-ray emission provides evidence for superfluidity in neutron stars but it is hard to conclude about the internal composition

Cooling of Cassiopeia A

The recent monitoring of the *fast* cooling of the young neutron star in Cassiopeia A provides strong evidence for neutron-star core superfluidity.

Page et al., PRL 106, 081101; Shternin et al., MNRAS 412, L108.

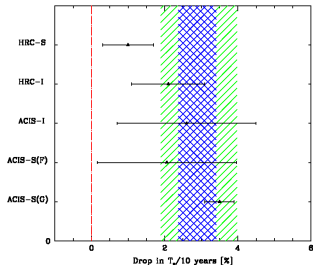


Superfluidity reduces the heat capacity and neutrino emissivities but also opens new channels of neutrino emission.

Cooling of Cassiopeia A

However, a more recent analysis of observational data from all detectors suggests that the cooling rate might be slower.

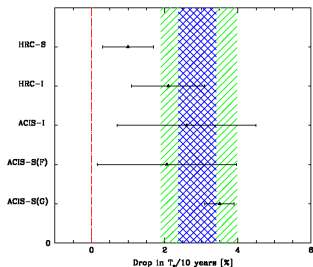
Elshamouty et al., ApJ 777, 22 (2013).



Cooling of Cassiopeia A

However, a more recent analysis of observational data from all detectors suggests that the cooling rate might be slower.

Elshamouty et al., ApJ 777, 22 (2013).



Moreover, alternative scenarios have been proposed.

Blaschke, Grigorian, Voskresensky, PRC88, 065805 (2013)

Bonanno, Baldo, Burgio, Urpin, A&A 561, L5 (2014)

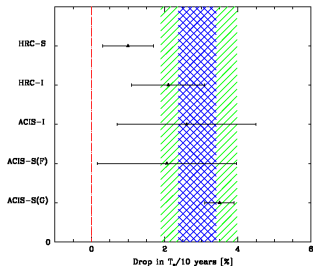
Negreiros, Schramm, Weber, Phys. Lett. B718, 1176 (2013)

Sedrakian, A&A 555, L10 (2013)

Cooling of Cassiopeia A

However, a more recent analysis of observational data from all detectors suggests that the cooling rate might be slower.

Elshamouty et al., ApJ 777, 22 (2013).



Moreover, alternative scenarios have been proposed.

Blaschke, Grigorian, Voskresensky, PRC88, 065805 (2013)

Bonanno, Baldo, Burgio, Urpin, A&A 561, L5 (2014)

Negreiros, Schramm, Weber, Phys. Lett. B718, 1176 (2013)

Sedrakian, A&A 555, L10 (2013)

Still, most scenarios require superfluidity and/or superconductivity in neutron stars.

Neutron star formation and cooling

Due to its relatively low neutrino emissivity, the crust of a newly-born neutron star cools less rapidly than the core and thus stays hotter.

The thermal relaxation time depends on the crust physics:

$$t_W \simeq (\Delta R)^2 \left[1 - \frac{2GM}{R} \right]^{-3/2} \frac{C_{\text{tot}}}{\kappa}$$

C_{tot} is the total heat capacity

κ is the thermal conductivity

Gnedin et al., MNRAS 324, 725 (2001).

Neutron star formation and cooling

Due to its relatively low neutrino emissivity, the crust of a newly-born neutron star cools less rapidly than the core and thus stays hotter.

The thermal relaxation time depends on the crust physics:

$$t_W \simeq (\Delta R)^2 \left[1 - \frac{2GM}{R} \right]^{-3/2} \frac{C_{\text{tot}}}{\kappa}$$

C_{tot} is the total heat capacity

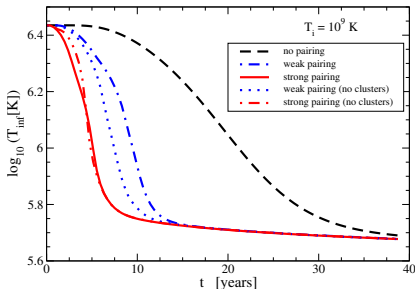
κ is the thermal conductivity

Gnedin et al., MNRAS 324, 725 (2001).

Neutron pairing suppresses the neutron heat capacity thus reducing t_W

Fortin et al., PRC 82, 065804 (2010)

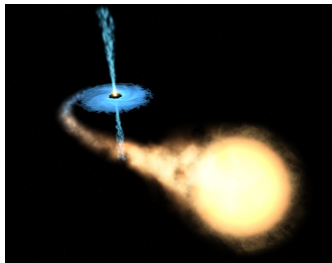
But so far no such young neutron stars have been observed; they are probably hidden by the expanding supernova envelopes.



X-ray binaries

Neutron stars in X-ray binaries may be **heated as a result of the accretion of matter** from the companion star (see Pawel Haensel's lecture).

The accretion of matter onto the surface of the neutron star triggers thermonuclear fusion reactions which can become explosive, giving rise to **X-ray bursts**.

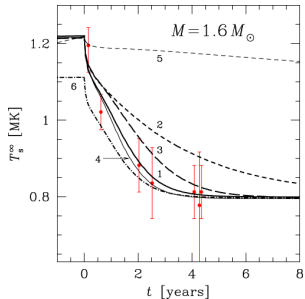


In quasipersistent soft X-ray transients (SXT), accretion outbursts are followed by **long period of quiescence** during which the accretion rate is much lower. In some cases, the period of accretion can last long enough for the crust to be **heated out of equilibrium with the core**.

Thermal relaxation of soft x-ray transients

The thermal relaxation during the quiescent state has been recently monitored for a few accreting neutron stars.

D. Page & S. Reddy in "Neutron Star Crust", edited by C. A. Bertulani and J. Piekarewicz, Nova Science Publishers, Inc. (New York, 2012), pp.281-308



Example: KS 1731–260

Curves 1,3,4 : crystalline crust with neutron superfluidity

Curve 2 : crystalline crust without neutron superfluidity

Curve 5 : amorphous crust with neutron superfluidity

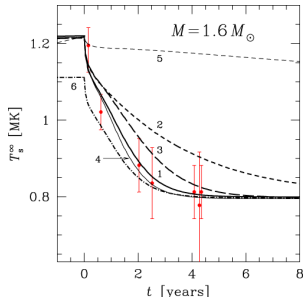
Shternin et al., Mon. Not. R. Astron. Soc.382(2007), L43.

Brown and Cumming, ApJ698 (2009), 1020.

Thermal relaxation of soft x-ray transients

The thermal relaxation during the quiescent state has been recently monitored for a few accreting neutron stars.

D. Page & S. Reddy in "Neutron Star Crust", edited by C. A. Bertulani and J. Piekarewicz, Nova Science Publishers, Inc. (New York, 2012), pp.281-308



Example: KS 1731–260

Curves 1,3,4 : crystalline crust with neutron superfluidity

Curve 2 : crystalline crust without neutron superfluidity

Curve 5 : amorphous crust with neutron superfluidity

Shternin et al., Mon. Not. R. Astron. Soc.382(2007), L43.

Brown and Cumming, ApJ698 (2009), 1020.

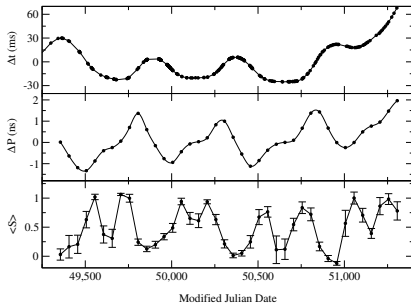
Observations of SXT provide evidence of superfluidity in the inner crust of a neutron star. But there are also puzzles (see Pawel Haensel's lecture).

Neutron star precession

Long-term cyclical variations of order months to years have been reported in a few neutron stars: Her X-1 (accreting neutron star), the Crab pulsar, PSR 1828–11, PSR B1642–03, PSR B0959–54 and RX J0720.4–3125.

Example: Time of arrival residuals, period residuals, and shape parameter for PSR 1828–11

Stairs et al., Nature 406(2000),484.



These variations have been interpreted as the signature of **neutron star precession**.

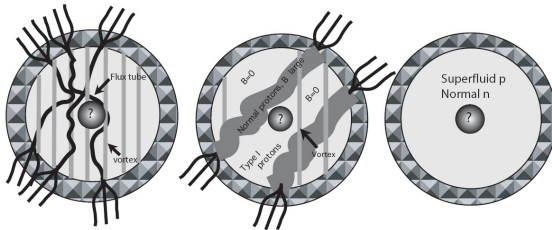
Precession and superfluidity

For a non-superfluid star with deformation $\epsilon = \Delta I / I$,

$$P_{\text{prec}} = \frac{P}{\epsilon} \gg P$$

For a superfluid star with pinned vortices

$$P_{\text{prec}} = \frac{I_{\text{pin}}}{I} P \ll P$$



Link, Astrophys. Space Sci.308,435 (2007)

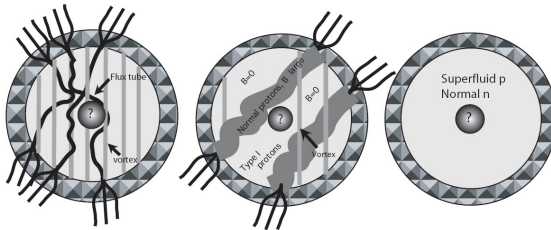
Precession and superfluidity

For a non-superfluid star with deformation $\epsilon = \Delta I/I$,

$$P_{\text{prec}} = \frac{P}{\epsilon} \gg P$$

For a superfluid star with pinned vortices

$$P_{\text{prec}} = \frac{I_{\text{pin}}}{I} P \ll P$$



Link, Astrophys. Space Sci.308,435 (2007)

Observations of precession could thus shed light on superfluidity. On the other hand, precession may trigger instabilities that could unpin vortices.

Glampedakis, Andersson, Jones, PRL 100, 081101 (2008).

Asteroseismology of neutron stars

The presence of superfluids and superconductors in neutron stars leads to the existence of new oscillations modes.

In the simplest two-fluid model, there exists two families of modes:

- "normal" modes (comoving fluids)
- "superfluid" modes (countermoving fluids)

Asteroseismology of neutron stars

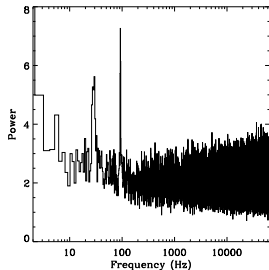
The presence of superfluids and superconductors in neutron stars leads to the existence of new oscillations modes.

In the simplest two-fluid model, there exists two families of modes:

- "normal" modes (comoving fluids)
- "superfluid" modes (countermoving fluids)

Quasiperiodic oscillations (QPOs) have been detected in the X-ray flux of giant flares from a few soft gamma-ray repeaters.

Example: SGR 1806–20
Strohmayer&Watts, ApJ653,593 (2006)



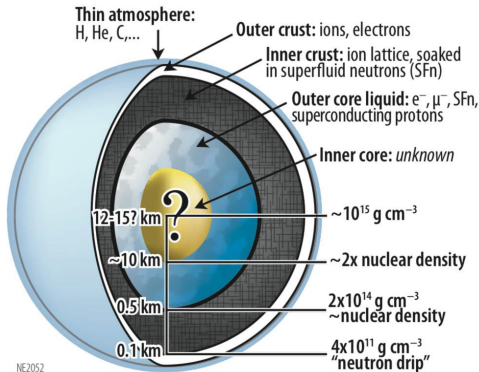
These QPOs are thought to be the signatures of **superfluid magneto-elastic oscillations**.

Gabler et al., PRL 111, 211102 (2013).

Summary

Nuclear superfluidity in neutron stars was predicted long before the discovery of pulsars, but many aspects still remain not very well understood (e.g. pairing phases, T_c , hydrodynamics).

What we know with confidence:



Fortunately, superfluidity leaves its imprint on various astrophysical phenomena (e.g. glitches, cooling, oscillations etc).

Bibliography

List of some references about superfluidity and superconductivity in compact stars:

Books/Lecture notes:

- *Novel Superfluids*, ed. Bennemann&Ketterson (Oxford University Press, 2015)
- Schmitt, Lecture Notes in Physics 888 (Springer, 2015).
- *50 years of nuclear BCS*, ed. Broglia&Zelevinsky (World Scientific, 2013)
- Sedrakian & Clark, in *Pairing in Fermionic Systems* (World Scientific Publishing, 2006), p.135
- Carter, Lecture Notes in Physics 578, 54 (Springer, 2001)
- Lombardo& Schulze, Lecture Notes in Physics 578, 30 (Springer, 2001)

Reviews:

- Anglani et al., Rev. Mod. Phys.86, 509 (2014)
- Alford, Schmitt, Rajagopal, Schäfer, Rev. Mod. Phys.80, 1455 (2008)
- Chamel & Haensel, Living Rev. Relativity 11, 10 (2008)
- Andersson & Comer, Living Rev. Relativity 10 (2007), 1
- Baldo, Saperstein, Tolonnikov, Nucl.Phys. A 749, 42c (2005)
- Dean & Hjorth-Jensen, Rev. Mod. Phys.75, 607 (2003)